

L-432

ACR No. 3F18

NATIONAL ADVISORY COMMITTEE FOR AERONAUTICS

# WARTIME REPORT

ORIGINALLY ISSUED

June 1943 as  
Advance Confidential Report 3F18

WIND-TUNNEL TESTS OF AILERONS AT VARIOUS SPEEDS

II - AILERONS OF 0.20 AIRFOIL CHORD AND TRUE CONTOUR

WITH 0.60 AILERON-CHORD SEALED INTERNAL BALANCE

ON THE NACA 66,2-216 AIRFOIL

By H. G. Denaci and J. D. Bird

Langley Memorial Aeronautical Laboratory  
Langley Field, Va.



WASHINGTON

NACA WARTIME REPORTS are reprints of papers originally issued to provide rapid distribution of advance research results to an authorized group requiring them for the war effort. They were previously held under a security status but are now unclassified. Some of these reports were not technically edited. All have been reproduced without change in order to expedite general distribution.



L-432

NATIONAL ADVISORY COMMITTEE FOR AERONAUTICS

ADVANCE CONFIDENTIAL REPORT

WIND-TUNNEL TESTS OF AILERONS AT VARIOUS SPEEDS  
II - AILERONS OF 0.20 AIRFOIL CHORD AND TRUE CONTOUR  
WITH 0.60 AILERON-CHORD SEALED INTERNAL BALANCE  
ON THE NACA 66,2-216 AIRFOIL

By H. G. Denaci and J. D. Bird

SUMMARY

Hinge-moment, lift, pressure difference across the balance, and pressure-distribution measurements were made in the two-dimensional test section of the stability tunnel on a 0.60 aileron-chord sealed internal-balance aileron on the NACA 66,2-216,  $a = 1.0$  airfoil.

The primary object of these tests was to determine the effect of speed on the action of this aileron. The airspeed was varied from 160 to 360 miles per hour, corresponding to Mach numbers of approximately 0.197 to 0.475, respectively. The vent gap was varied from 0.0025 wing chord to 0.0100 wing chord.

The variations in section hinge-moment coefficient, section lift coefficient, and pressure coefficient across the balance with Mach number, angle of attack, aileron angle, and vent gap are given graphically. The pressure coefficient across the balance has been given in order that the desired amount of balance can be more readily obtained. Cross plots have also been included to show the general effect of changes in Mach number and vent gap.

An increase of speed in the range tested generally increased the slopes of the curves of hinge-moment coefficient and lift coefficient and also caused a considerable decrease of the unstalled range of the aileron.

## INTRODUCTION

The forms of ailerons in use today have given performance that was satisfactory according to previous requirements. With the development of current combat airplanes, however, large increases in speed and wing area, together with the demand for higher rolling velocities, have introduced difficulties such as overbalance at high speeds on some of the existing aileron installations.

This difficulty with balance is apparently the result of compressibility effects on the almost exact balance required at high speed. It has been considered desirable, therefore, to reinspect some of the currently used or recently proposed balance arrangements from these considerations. The NACA is therefore undertaking a study of some of the more promising aileron forms at higher speeds than those employed in previous development. As reported in reference 1, an aileron of 0.20 airfoil chord with 0.35 aileron-chord blunt-nose balance has already been tested. The present investigation was made to determine the effect of speed, up to a Mach number of 0.475, on the section characteristics of a 0.20 airfoil-chord aileron of true contour with 0.60 aileron-chord sealed internal balance on the NACA 66,2-216,  $a = 1.0$  airfoil, and also to determine the effect of variation of vent gap on the aerodynamic characteristics. The 0.60 aileron-chord balance was chosen because unpublished data from Ames Aeronautical Laboratory has indicated that satisfactory hinge-moment characteristics would be obtained on this type of aileron with this airfoil section.

Curves showing the variations of aileron section hinge-moment coefficient, section lift coefficient, and pressure coefficient across the balance with aileron angle are plotted for five airspeeds that correspond to Mach numbers of 0.197 to 0.475. Cross plots showing typical effects of various parameters on the aerodynamic characteristics are included for comparisons. A comparison of this aileron with the blunt-nose aileron of reference 1 on the same airfoil is also included.

## SYMBOLS

The coefficients and symbols used in this paper are defined as follows:

$c_l$	airfoil section lift coefficient $\left(\frac{l}{qc}\right)$
$\Delta c_l$	increment of airfoil section lift coefficient
$c_{h_a}$	aileron section hinge-moment coefficient $\left(\frac{h_a}{qc_a s}\right)$
$\Delta P$	increment of pressure coefficient across balance (pressure below balance minus pressure above balance divided by dynamic pressure)

where

$l$	airfoil section lift
$h_a$	aileron section hinge moment
$c$	chord of basic airfoil, including aileron
$c_a$	chord of aileron behind hinge axis
$q$	dynamic pressure $\left(\frac{1}{2} \rho V^2\right)$
$V$	absolute velocity of air stream
$\rho$	mass density of air
and	
$\alpha_0$	angle of attack of airfoil for infinite aspect ratio
$\delta_a$	aileron deflection with respect to airfoil
$M$	Mach number

$\left(\frac{\partial c_{h_a}}{\partial \delta_a}\right)_{\alpha_0}$  slope of  $c_{h_a}$  against  $\delta_a$  at constant  $\alpha_0$

$\left(\frac{\partial c_{h_a}}{\partial \alpha_0}\right)_{\delta_a}$  slope of  $c_{h_a}$  against  $\alpha_0$  at constant  $\delta_a$

$\left(\frac{\partial \Delta P}{\partial \delta_a}\right)_{\alpha_0}$  slope of  $\Delta P$  against  $\delta_a$  at constant  $\alpha_0$

$\left(\frac{\partial c_l}{\partial \delta_a}\right)_{\alpha_0}$  slope of  $c_l$  against  $\delta_a$  at constant  $\alpha_0$

$\left(\frac{\partial c_l}{\partial \alpha_0}\right)_{\delta_a=0}$  slope of  $c_l$  against  $\alpha_0$  at  $\delta_a = 0^\circ$

#### APPARATUS AND MODEL

Tests were made in the two-dimensional test section of the stability tunnel. This section is rectangular, 6 feet high and 2.5 feet wide. Air velocities up to 400 miles per hour are possible in this section. Figure 1 is a photograph of the test section with a model in place.

The model investigated had an NACA 66,2-216,  $a = 1.0$  airfoil section of 2-foot chord. Table I gives the airfoil ordinates. The wing portion of the model was made of laminated mahogany. The 0.20c aileron of true contour with 0.60c<sub>a</sub> sealed internal balance was made of steel. Cover plates were also of steel, faired to the airfoil contour, and the vent gap was varied by use of cover plates of different lengths. The seal was made of impregnated cotton and extended completely across the airfoil span. Clearance at the ends of the balance was kept to a minimum and sealed with grease to prevent leakage. Figure 2 is a sketch of the aileron tested.

The aileron was supported at the ends by ball bearings housed in steel end plates attached to the airfoil. The airfoil was fixed into circular end disks, which were flush with the tunnel walls with about 1/8-inch clearance between the aileron and the end disks.

The angle of attack was changed by rotating the end disks. Aileron angles were varied and hinge moments were measured by a calibrated spring-torque balance and sector system. Lift was measured by an integrating manometer connected to orifices in the floor and ceiling of the tunnel. The integrating manometer was calibrated against lift obtained by pressure-distribution measurements on the airfoil. Pressure orifices were located on the center line of the wing and aileron and the pressure distribution was recorded by photographing the multiple-tube manometer. Pressure openings were located under the cover plates on each side of the balance near the center line and the pressure difference across the balance was read along with the lift and hinge-moment readings.

## TESTS

Tests were made with vent gaps of 0.0025c, 0.0050c, and 0.0100c. Hinge moments, lift, and the pressure difference across the balance were measured. Pressure distributions were recorded photographically.

Tests with each vent width were made at five Mach numbers in a range between 0.197 and 0.475. The lowest value of  $M$  corresponds to a Reynolds number of 2,800,000 and the highest value to a Reynolds number of about 6,700,000. Reynolds number based on standard atmospheric conditions plotted against test Mach number is given as figure 3. Tests were made at angles of attack of  $-5^\circ$ ,  $0^\circ$ ,  $5^\circ$ , and  $10^\circ$ . For each angle of attack, readings were taken at the following aileron angles:  $0^\circ$ ,  $\pm 2^\circ$ ,  $\pm 5^\circ$ ,  $\pm 7^\circ$ ,  $\pm 10^\circ$ ,  $\pm 16^\circ$ ,  $\pm 18^\circ$ , and  $\pm 20^\circ$ . The highest value of Mach number could not be attained at the large angles of attack with large aileron deflections because of limited tunnel power.

Pressure-distribution records were made at Mach numbers of 0.198, 0.358, and 0.475 for angles of attack of  $0^\circ$  and  $10^\circ$ . At each angle of attack the aileron settings were  $0^\circ$ ,  $\pm 5^\circ$ ,  $\pm 10^\circ$ , and  $\pm 16^\circ$ .

## PRECISION

Angles of attack were set to within  $\pm 0.1^\circ$  and aileron angles to within  $\pm 0.3^\circ$ . The hinge-moment coefficients could be repeated to within  $\pm 0.003$ , lift coefficients to within  $\pm 0.01$ , and pressure coefficient across the balance to within  $\pm 0.03$ .

Corrections for tunnel-wall effects were applied to the lift coefficients and to the angles of attack. The corrections applied are:

$$c_l = [1 - Y (1 + 2\beta)] c_l'$$

$$\alpha_o = (1 + Y) \alpha_o'$$

where

$$Y = \frac{\pi^2}{48} \left( \frac{c}{h} \right)^2$$

$\beta = 0.304$  (theoretical factor for NACA 66,2-216,  $a = 1.0$  airfoil)

$h$  height of tunnel

$c_l'$  measured lift coefficient

$\alpha_0'$  uncorrected or geometric angle of attack

The values used are:

$$c_l = 0.963 c_l'$$

$$\alpha_0 = 1.023 \alpha_0'$$

No corrections were applied to the section hinge-moment coefficients or to the pressure coefficient across the balance.

The spring-balance method used in this report for obtaining section hinge-moment coefficients was checked for a number of cases by the pressure-distribution method and the comparison is given in figure 4. The variations shown are probably due to the fact that the spring balance measures the moment of the entire aileron, which includes effects of boundary layer at the tunnel wall and of gaps at the ends of the aileron as well as any cross flow over the aileron. The pressure distribution, however, gives the hinge moment of one section of the aileron and is subject to errors in fairing the pressure-distribution diagrams. The majority of the points shown are within the accuracy of the spring-balance measuring system.

## RESULTS AND DISCUSSION

The results of this investigation are presented graphically in figures 5 to 18. In order that individual plots may be more easily identified, table II gives the figure number, variations shown, test Mach number, and vent gap.

### Hinge Moments of the Aileron

The effect of an increase of the airspeed from a Mach number  $M$  of 0.2 to 0.47 was appreciable on the curves of section hinge-moment coefficient  $c_{h_a}$  plotted against

aileron angle  $\delta_a$ . A study of figure 5 shows that the range in which  $c_{ha}$  continues to increase linearly with  $\delta_a$  decreases with increase of speed and that, in this linear range, the slope of these curves increased with speed. In order that the effect of change of airspeed and vent gap on

$\left(\frac{\partial c_{ha}}{\partial \delta_a}\right)_{\alpha_0}$  may be more readily seen, this parameter has been

plotted against Mach number in figure 6 and against vent gap in figure 7. Because the hinge-moment-coefficient curves often changed slope at zero aileron angle, values of  $c_{ha}$  at aileron angles of  $\pm 5^\circ$  were arbitrarily used to determine the slope. It is evident that, in the range tested,

$\left(\frac{\partial c_{ha}}{\partial \delta_a}\right)_{\alpha_0}$  becomes greater negatively with increase of  $M$

for all but the  $10.2^\circ$  angle of attack  $\alpha_0$ . Part of this change may be due to Reynolds number. The change in slope when  $\alpha_0 = 10.2^\circ$  at  $M = 0.35$  is not understood but is believed to be associated with the attainment of critical speeds over the forward position of the airfoil at this angle of attack.

Changes of the vent gap from 0.0025c to 0.0100c also caused a general negative increase in  $\left(\frac{\partial c_{ha}}{\partial \delta_a}\right)_{\alpha_0}$ . This result is in agreement with the results given in reference 2, in which the vent width was varied. There was no noticeable change of the stalled range of the aileron with vent gap. (See figs. 5 and 7.)

With the 0.60c<sub>a</sub> balance tested,  $\left(\frac{\partial c_{ha}}{\partial \delta_a}\right)_{\alpha_0}$  was positive at  $\alpha_0 = 0^\circ$  over part of the speed range, and overbalance is indicated. One requirement for balance is that

$\left(\frac{\partial c_{ha}}{\partial \delta_a}\right)_{\alpha_0}$  be negative, but this condition is not sufficient

for balance when the change in angle of attack due to rolling is considered. In these tests  $\left(\frac{\partial c_{ha}}{\partial \delta_a}\right)_{\alpha_0}$  was negative

at all angles of attack at high speed; yet, if the rolling condition is considered when stick forces are estimated, the ailerons may be overbalanced at all speeds for a large range of aileron deflections.

If the pressure difference across the balance is assumed to be equal for all points along the balance, it is reasonable to expect that the  $c_{h_a}$  can be predicted for any other amount of balance. This fact is substantiated by the data and discussion in reference 3. The following relation based on the geometry of the balance parts has been derived:

$$c_{h'} = c_{h_a} - \left[ 0.1624 - (x - 0.1875) \left( \frac{x - 0.1875}{2} + 0.1875 \right) \right] \Delta P \quad (1)$$

where

$c_{h'}$  aileron section hinge-moment coefficient of an aileron of  $x$  balance

$x$  amount of balance in fraction of aileron chord; for plain aileron,  $x = 0.1875$

The pressure coefficient across the balance  $\Delta P$  is given in figure 8 for conditions identical to those at which the hinge moments were measured. The variation of

$\left( \frac{\partial \Delta P}{\partial \delta_a} \right)_{\alpha_0}$  with Mach number in the range tested is small.

Absolute values of  $\Delta P$  at large aileron angles were lower at high airspeeds than at low airspeeds. The highest values of  $\Delta P$  were generally obtained with the smallest gap that was used, which is as expected.

From the use of  $c_{h_a}$  and  $\Delta P$  obtained from the 0.0050c vent gap at  $M = 0.358$  and formula (1), the hinge-moment coefficients for a plain sealed aileron were calculated and are given in figure 9. The curves of hinge-moment coefficient computed for a plain sealed aileron are nearly linear throughout the aileron range.

Data from figure 5 have been cross-plotted to show the variation of  $c_{h_a}$  with angle of attack for three representative aileron angles in figure 10. The average incre-

ment of  $c_{ha}$  for  $\alpha_0 = -5.1^\circ$  to  $10.2^\circ$  is  $-0.09$ , which gives an average value of  $\left(\frac{\partial c_{ha}}{\partial \alpha_0}\right)_{\delta_a}$  of  $-0.0059$ . Specific values of  $\left(\frac{\partial c_{ha}}{\partial \alpha_0}\right)_{\delta_a}$  may vary widely from  $-0.0059$ .

### Lift

The airfoil section lift coefficient  $c_l$  plotted against angle of attack for the various speeds and vent gaps that were tested are given in figure 11 for zero aileron angle.

The parameter  $\left(\frac{\partial c_l}{\partial \alpha_0}\right)_{\delta_a=0}$  was taken between

$\alpha_0$  of  $-5^\circ$  and  $0^\circ$ . A characteristic of this low-drag airfoil section is that separation takes place between an  $\alpha_0$  of  $2^\circ$  and  $4^\circ$ , and a change in the lift curve results. More information on this phenomenon is given in reference 4.

The parameter  $\left(\frac{\partial c_l}{\partial \alpha_0}\right)_{\delta_a=0}$  was plotted against  $M$  in figure 12, and a change of  $\left(\frac{\partial c_l}{\partial \alpha_0}\right)_{\delta_a=0}$  of  $0.017$  was obtained for

the vent gaps of  $0.0025c$  and  $0.0050c$  for a change of  $M$  between  $0.2$  and  $0.475$ . Glauert and Ackeret have shown that the lift curve slope should vary with  $M$  as  $\frac{1}{\sqrt{1-M^2}}$ .

This variation is shown in figure 12 by using an arbitrary lift slope of  $0.099$  at  $M = 0$  in such a way that the theoretical increase of lift slope passes through the measured value for the  $0.0025c$  and  $0.0050c$  vent gaps at  $M = 0.2$ . A comparable change in  $M$  of  $0.011$  is obtained by this method. The observed difference between the two curves is believed to be due to the fact that Reynolds number may have an appreciable effect on the slope of the lift curve, as is indicated by the data given in reference 4 for this airfoil section, and to the fact that the wind-tunnel correction which was applied neglected compressibility effects. The vent gaps of  $0.0025c$  and  $0.0050c$  gave identical results, whereas the  $0.0100c$  vent gap showed a consistently lower lift-curve slope. This difference may be due to misalignment of the cover plates.

Plots of section lift coefficient  $c_l$  against aileron

angle (fig. 13) show that the most noticeable effect of an increase in the airspeed is a decrease of the angle at which the slope of the lift curve changes. In order to avoid confusion the curves in figure 13 have been faired through the points for a Mach number of 0.358 only. The

parameter  $\left(\frac{\partial c_l}{\partial \delta a}\right)_{\alpha_0}$  obtained from values of  $c_l$  at  $\delta a$

of  $\pm 5^\circ$  is plotted against  $M$  in figure 14 and against

vent gap in figure 15. A small increase of  $\left(\frac{\partial c_l}{\partial \delta a}\right)_{\alpha_0}$  was

noticed with increase of airspeed in the range tested for all but the  $10.2^\circ$  angle of attack. Variations of the slope with vent gap were too irregular to show any defi-

nite trends. The values of  $\left(\frac{\partial c_l}{\partial \delta a}\right)_{\alpha_0}$  obtained in this

test are in close agreement with the values obtained from reference 4 for a 20-percent chord, plain scaled flap on the same airfoil and at approximately the same Reynolds number.

#### Control-Force Criterion

The variation of  $\Delta c_{ha} \delta a$  with  $\Delta c_l$  is a control-force criterion that takes into account not only the reduction in  $\Delta c_{ha}$  but also the possible reduction in  $\Delta c_l$  (for a given deflection) that may be caused by the balancing device. Even though  $\Delta c_{ha}$  may be reduced considerably, if in doing so it is necessary to move the control surface through a very large angle (decreasing the stick leverage of the ailerons), the product  $\Delta c_{ha} \delta a$  may be increased somewhat to obtain the same  $\Delta c_l$ . The criterion as used herein is strictly valid only at the instant that the aileron is deflected. The use of this criterion for computing stick forces during a roll will give an erroneous indication of these forces because differences in

$\left(\frac{\partial c_{ha}}{\partial \alpha_0}\right)_{\delta a}$  for the ailerons that are being compared are not taken into account.

Figure 16 shows this criterion compared at various

Mach numbers. The effect of an increase in speed is small except at large aileron deflections; in this case the control-force criterion is generally lower at low speeds than at high speeds. Variations with vent gap when compared by this criterion were small (fig. 17); the 0.0025c and 0.0050c vent gaps, however, gave slightly better results than the 0.0100c vent gap.

The blunt nose balance aileron with 0.02c radii and 0.0055 gap reported in reference 1 is compared in figure 18 with the aileron tested in this investigation. It is evident that, when compared by this criterion, the internal-balance aileron tested had not only lower values of  $\Delta c_{h_a} \delta_a$  at specific values of  $\Delta c_l$  and less separation of these curves with angle of attack, but also higher values of  $\Delta c_l$  obtainable with aileron deflection, than the 0.35c<sub>a</sub> blunt nose balance aileron on this airfoil.

A noticeable difference between the two ailerons, not shown in any of the figures, is that the oscillations that occurred at the transition point between the stalled and unstalled range on the blunt nose aileron were either not present or were so small as to be unnoticed on the internal-balance aileron. A possible explanation for this phenomenon is that the stall was not as clearly defined on the internal-balance type and, as discussed in reference 3, there may be a heavy damping of oscillations with the internal balance.

### CONCLUSIONS

The results of this investigation of an internal-balance aileron of 0.20 airfoil chord and true contour with a 0.60 aileron-chord balance tested on the NACA 66,2-216,  $\alpha = 1.0$  airfoil section indicate the following general conclusions:

1. Increasing the airspeed up to a Mach number of 0.475 noticeably increased the slope of the curves of the hinge-moment coefficient and of the airfoil lift coefficient but, at the same time, considerably decreased the unstalled range of the aileron.

2. Changes of the vent gap from 0.0025 chord to 0.0100 chord had little effect on the aerodynamic characteristics; best aerodynamic characteristics, however, were obtained with a vent gap of 0.0050 chord or less.

3. A 0.60 aileron chord sealed internal balance on this aileron causes overbalance at zero angle of attack for low airspeeds; moreover, when the change in angle of attack due to rolling is considered, the aileron may be overbalanced at all speeds for a large range of aileron deflections.

4. The internal-balance aileron tested had much better aerodynamic characteristics than the blunt nose ailerons tested on the same airfoil.

Langley Memorial Aeronautical Laboratory,  
National Advisory Committee for Aeronautics,  
Langley Field, Va.

#### REFERENCES

1. Letko, W., Denaci, H. G., and Freed, C.: Wind-Tunnel Tests of Ailerons at Various Speeds. I - Ailerons of 0.20 Airfoil Chord and True Contour with 0.35 Aileron Chord Extreme Blunt Nose Balance on the NACA 66,2-216 Airfoil. NACA ACR No. 3F11, 1943.
2. Sears, Richard I., and Hoggard, H. Page, Jr.: Wind-Tunnel Investigation of Control-Surface Characteristics. XI - Various Large Overhang and Internal-Type Aerodynamic Balances for a Straight-Contour Flap on the NACA 0015 Airfoil. NACA ARR, Jan. 1943.
3. Irving, H. B., Batson, A. S., and Warsap, J. H.: Notes and Exploratory Experiments on the Aerodynamic Balancing of Controls. 4284 S. & C. 1093, British A.R.C. (British Confidential - U.S. Restricted), Nov. 27, 1939.
4. Jacobs, Eastman N., Abbott, Ira H., and Davidson, Milton: Supplement to NACA Advance Confidential Report, Preliminary Low-Drag-Airfoil and Flap Data from Tests at Large Reynolds Numbers and Low Turbulence. NACA (Loose leaf), March 1942.

TABLE I

ORDINATES FOR NACA 66,2-216,  $a = 1.0$  AIRFOIL

[Stations and ordinates in percent of wing chord]

Upper surface		Lower surface	
Station	Ordinate	Station	Ordinate
0	0	0	0
.401	1.230	.599	-1.130
.640	1.484	.860	-1.344
1.128	1.853	1.372	-1.644
2.362	2.560	2.638	-2.188
4.846	3.604	5.154	-2.972
7.340	4.428	7.660	-3.580
9.838	5.140	10.162	-4.106
14.845	6.276	15.155	-4.930
19.860	7.156	20.140	-5.564
24.879	7.844	25.121	-6.054
29.900	8.366	30.100	-6.422
34.924	8.736	35.076	-6.676
39.949	8.980	40.051	-6.838
44.974	9.092	45.026	-6.902
50.000	9.060	50.000	-6.854
55.025	8.875	54.975	-6.685
60.048	8.496	59.952	-6.354
65.067	7.862	64.933	-5.802
70.081	6.941	69.919	-4.997
75.087	5.860	74.913	-4.070
80.085	4.644	79.915	-3.052
85.075	3.395	84.925	-2.049
90.055	2.103	89.945	-1.069
95.028	.913	94.972	-.281
100.000	0	100.000	0
L.E. Radius = 1.575			

TABLE 1. - SUMMARY OF DATA FOR THE YEAR 1964			
Area	Population	Area	Population
1.01	1,000	1.02	1,000
1.03	1,000	1.04	1,000
1.05	1,000	1.06	1,000
1.07	1,000	1.08	1,000
1.09	1,000	1.10	1,000
1.11	1,000	1.12	1,000
1.13	1,000	1.14	1,000
1.15	1,000	1.16	1,000
1.17	1,000	1.18	1,000
1.19	1,000	1.20	1,000
1.21	1,000	1.22	1,000
1.23	1,000	1.24	1,000
1.25	1,000	1.26	1,000
1.27	1,000	1.28	1,000
1.29	1,000	1.30	1,000
1.31	1,000	1.32	1,000
1.33	1,000	1.34	1,000
1.35	1,000	1.36	1,000
1.37	1,000	1.38	1,000
1.39	1,000	1.40	1,000
1.41	1,000	1.42	1,000
1.43	1,000	1.44	1,000
1.45	1,000	1.46	1,000
1.47	1,000	1.48	1,000
1.49	1,000	1.50	1,000
1.51	1,000	1.52	1,000
1.53	1,000	1.54	1,000
1.55	1,000	1.56	1,000
1.57	1,000	1.58	1,000
1.59	1,000	1.60	1,000
1.61	1,000	1.62	1,000
1.63	1,000	1.64	1,000
1.65	1,000	1.66	1,000
1.67	1,000	1.68	1,000
1.69	1,000	1.70	1,000
1.71	1,000	1.72	1,000
1.73	1,000	1.74	1,000
1.75	1,000	1.76	1,000
1.77	1,000	1.78	1,000
1.79	1,000	1.80	1,000
1.81	1,000	1.82	1,000
1.83	1,000	1.84	1,000
1.85	1,000	1.86	1,000
1.87	1,000	1.88	1,000
1.89	1,000	1.90	1,000
1.91	1,000	1.92	1,000
1.93	1,000	1.94	1,000
1.95	1,000	1.96	1,000
1.97	1,000	1.98	1,000
1.99	1,000	2.00	1,000

TABLE II  
LIST OF PLOTTED RESULTS

Figure number	Variation shown	Mach number (approx.)	Vent gap
5	$c_{ha}$ against $\delta_a$	$\left\{ \begin{array}{l} 0.198, .290, \\ .358, .418, \\ .474 \end{array} \right.$	$\left\{ \begin{array}{l} (a) 0.0025c \\ (b) .0050c \\ (c) .0100c \end{array} \right.$
6	$\left( \frac{\partial c_{ha}}{\partial \delta_a} \right)_{\alpha_0}$ against M	Varies	0.0050c
7	$\left( \frac{\partial c_{ha}}{\partial \delta_a} \right)_{\alpha_0}$ against vent gap	0.198, .418	Varies
8	$\Delta P$ against $\delta_a$	$\left\{ \begin{array}{l} 0.198, .290, \\ .358, .418, \\ .474 \end{array} \right.$	$\left\{ \begin{array}{l} (a) 0.0025c \\ (b) .0050c \\ (c) .0100c \end{array} \right.$
9	$\left\{ \begin{array}{l} c_{ha} \text{ against } \delta_a \\ \text{(computed for 0.20c plain} \\ \text{aileron)} \end{array} \right.$	0.358	0.0050c
10	$c_{ha}$ against $\alpha_0$	0.198, .418	0.0050c
11	$c_l$ against $\alpha_0$	$\left\{ \begin{array}{l} 0.198, .290, \\ .358, .418, \\ .474 \end{array} \right.$	$\left\{ \begin{array}{l} 0.0025c \\ .0050c \\ .0100c \end{array} \right.$
12	$\left( \frac{\partial c_l}{\partial \alpha_0} \right)_{\delta_a}$ against M	Varies	$\left\{ \begin{array}{l} 0.0025c \\ .0050c \\ .0100c \end{array} \right.$
13	$c_l$ against $\delta_a$	$\left\{ \begin{array}{l} 0.198, .290, \\ .358, .418, \\ .474 \end{array} \right.$	$\left\{ \begin{array}{l} (a) 0.0025c \\ (b) .0050c \\ (c) .0100c \end{array} \right.$
14	$\left( \frac{\partial c_l}{\partial \delta_a} \right)_{\alpha_0}$ against M	Varies	0.0050c
15	$\left( \frac{\partial c_l}{\partial \delta_a} \right)_{\alpha_0}$ against vent gap	0.198, .418	Varies
16	$\left\{ \begin{array}{l} \Delta c_{ha} \delta_a \text{ against } \Delta c_l \\ \text{showing variation with} \\ \text{M} \end{array} \right.$	$\left\{ \begin{array}{l} 0.198, .290 \\ .358, .418 \\ .474 \end{array} \right.$	0.0050c
17	$\left\{ \begin{array}{l} \Delta c_{ha} \delta_a \text{ against } \Delta c_l \\ \text{showing variation with} \\ \text{vent gap} \end{array} \right.$	0.418	$\left\{ \begin{array}{l} 0.0025c \\ .0050c \\ .0100c \end{array} \right.$
18	$\left\{ \begin{array}{l} \Delta c_{ha} \delta_a \text{ against } \Delta c_l \\ \text{comparing aileron tested} \\ \text{with blunt nose type} \end{array} \right.$	0.198, .418	0.0050c

TABLE II

LIST OF FACTORS AFFECTING

Factor	Direction of Effect	Percentage Change
1. Temperature	Directly proportional	1.00%
2. Humidity	Inversely proportional	0.50%
3. Wind velocity	Directly proportional	0.25%
4. Air density	Inversely proportional	0.10%
5. Surface area	Directly proportional	0.75%
6. Friction coefficient	Inversely proportional	0.30%
7. Viscosity	Directly proportional	0.15%
8. Elasticity	Inversely proportional	0.05%
9. Conductivity	Directly proportional	0.40%
10. Permeability	Inversely proportional	0.20%
11. Porosity	Directly proportional	0.60%
12. Capillarity	Inversely proportional	0.35%
13. Cohesion	Directly proportional	0.12%
14. Adhesion	Inversely proportional	0.08%
15. Surface tension	Directly proportional	0.90%
16. Viscous resistance	Inversely proportional	0.45%
17. Elastic resistance	Directly proportional	0.22%
18. Compressibility	Inversely proportional	0.18%
19. Thermal expansion	Directly proportional	0.70%
20. Thermal contraction	Inversely proportional	0.32%

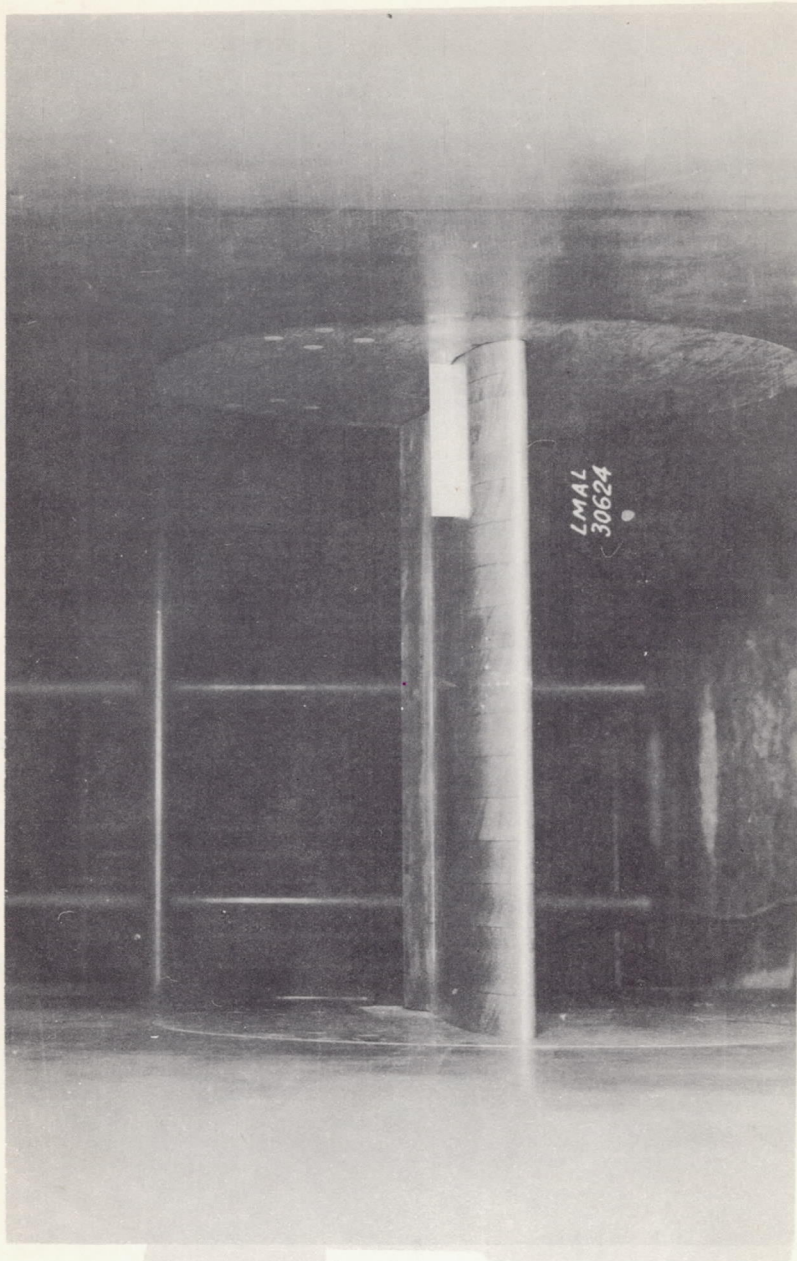


Figure 1.- Airfoil and aileron mounted in tunnel.



Vent gap

1	= $0.0025 c$
2	= $.0050 c$
3	= $.0100 c$

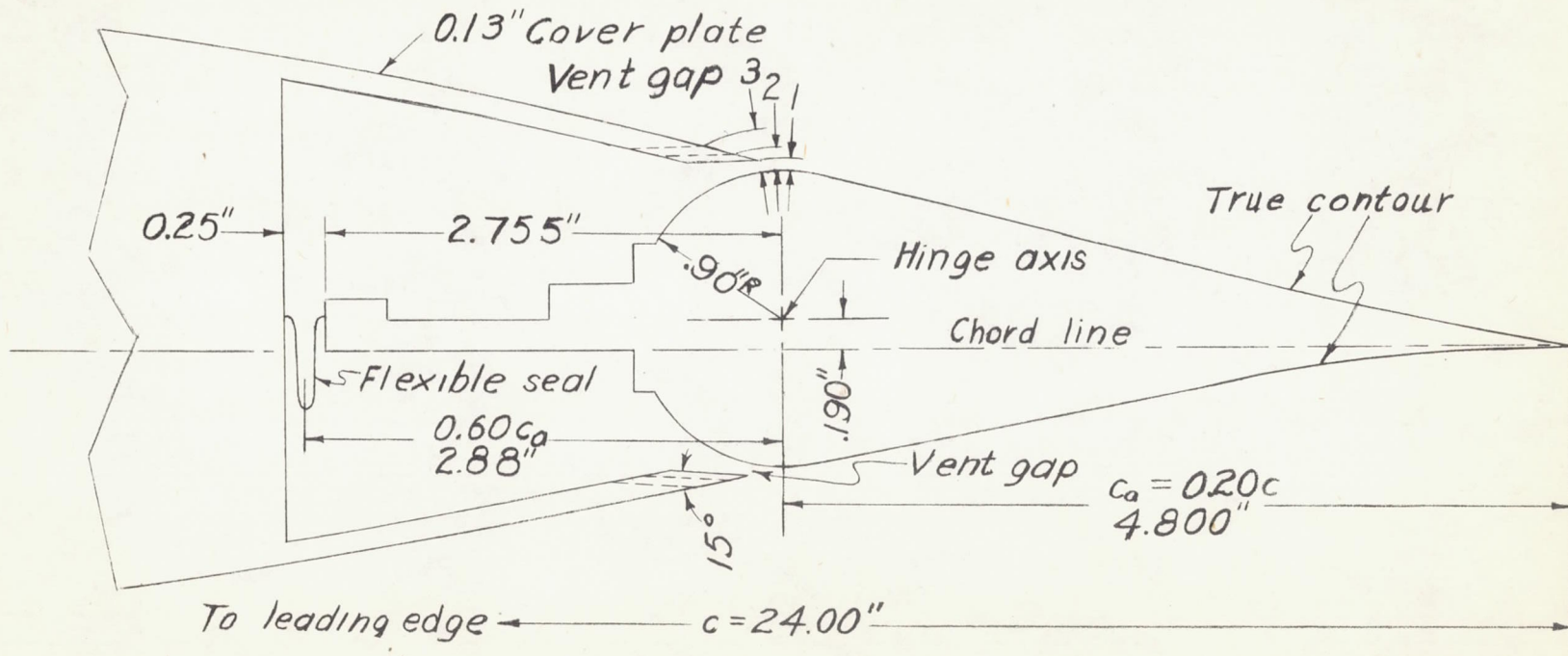


Figure 2.-Aileron section of the NACA 66,2-216; $\alpha=1.0$  airfoil tested with a  $0.20c$ ,  $0.60c_a$  sealed internal balance aileron of true contour.



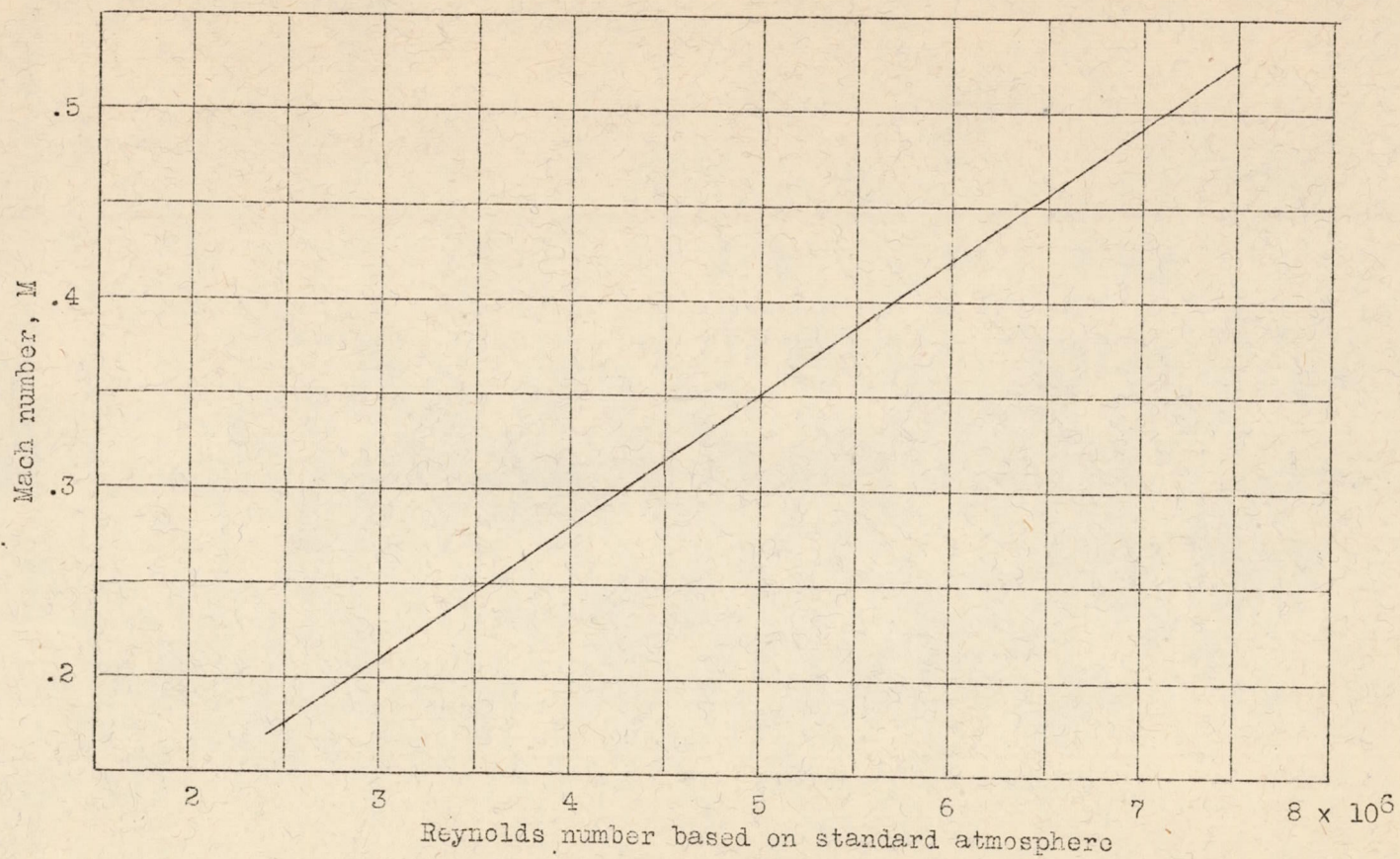


Figure 3.-- Reynolds number for values of Mach number for a 2-foot chord airfoil in the 2.5-by 6-foot test section of the stability tunnel.



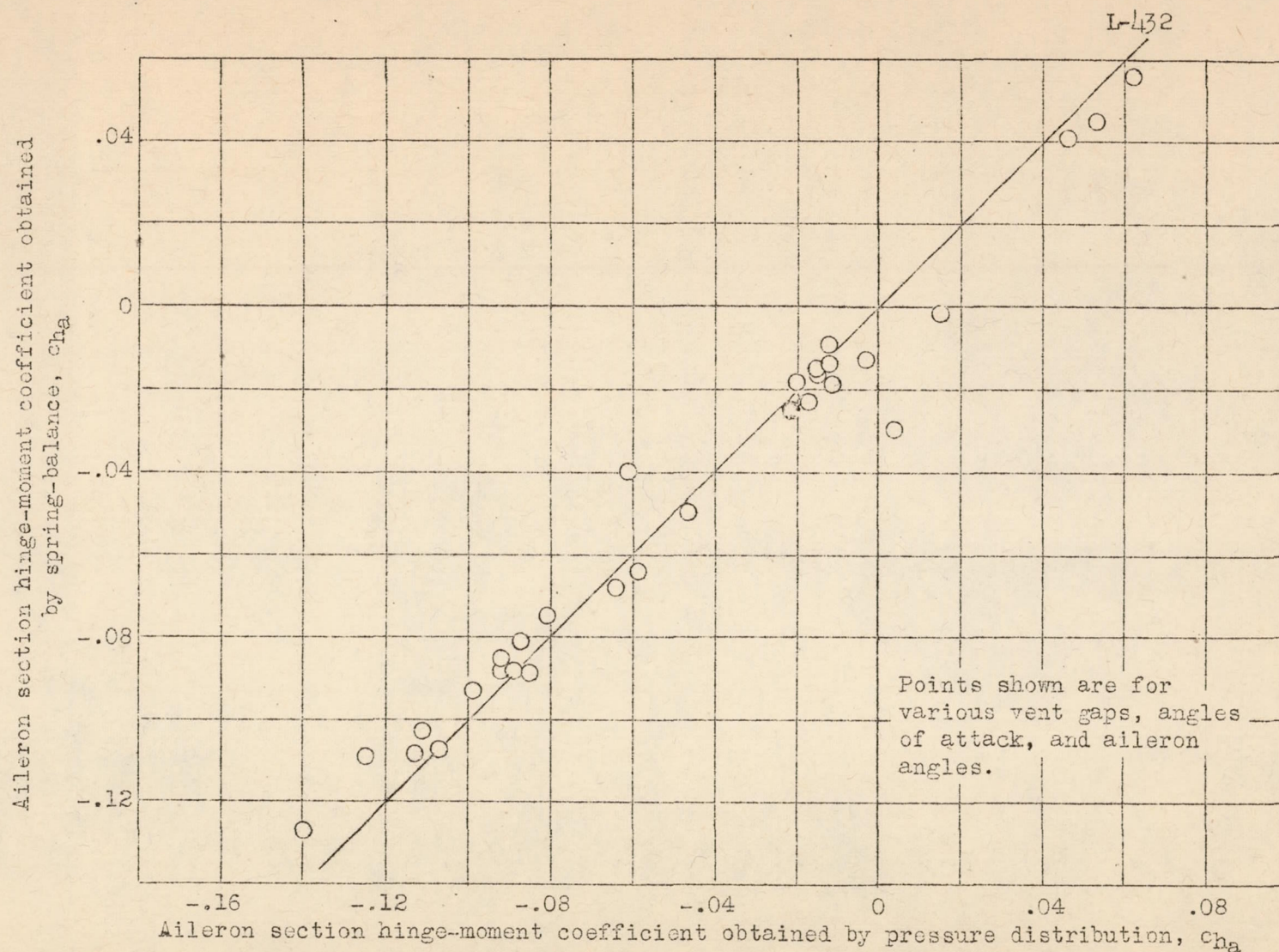
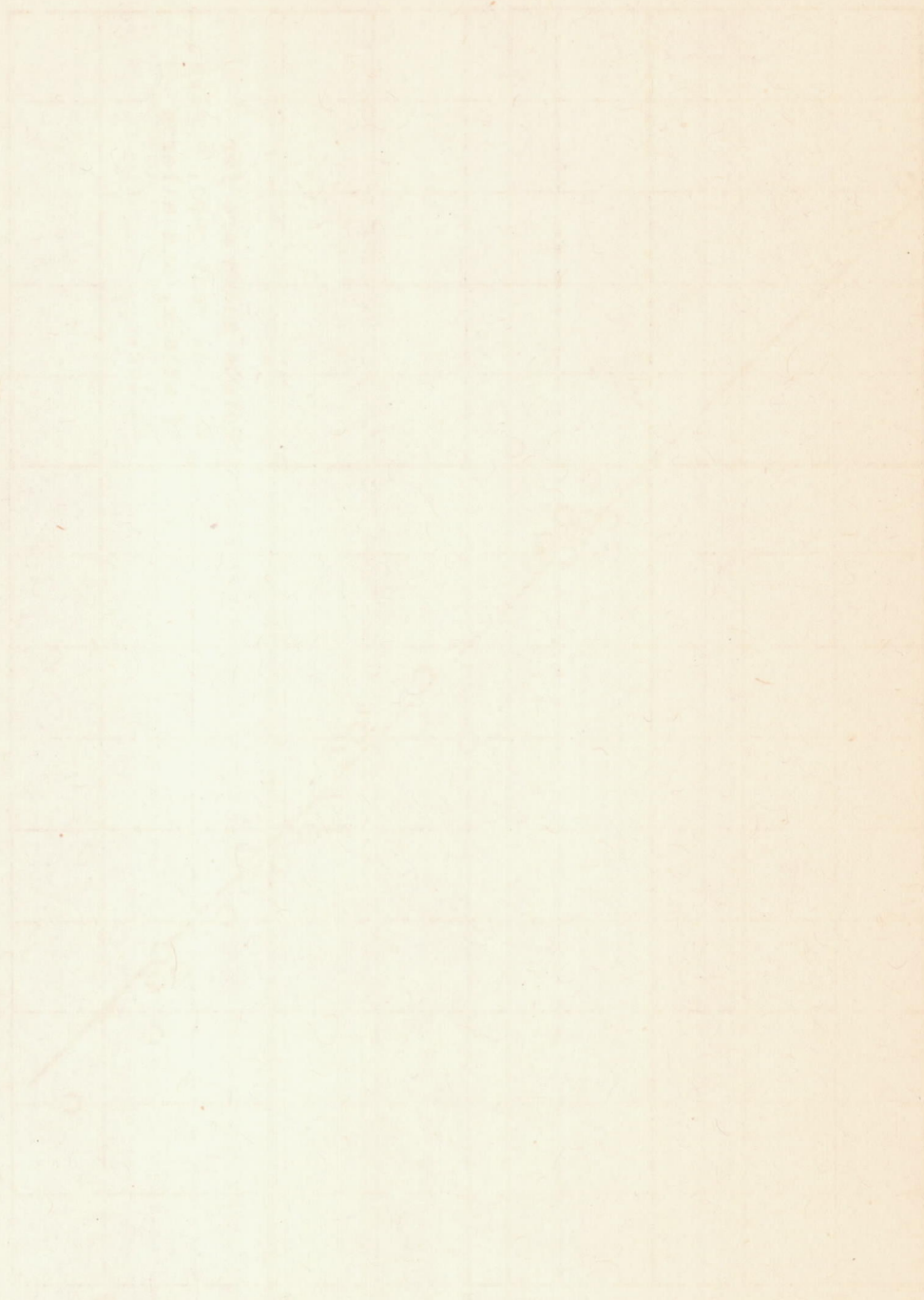


Figure 4.- A comparison between spring-balance and pressure distribution section hinge-moment coefficients.



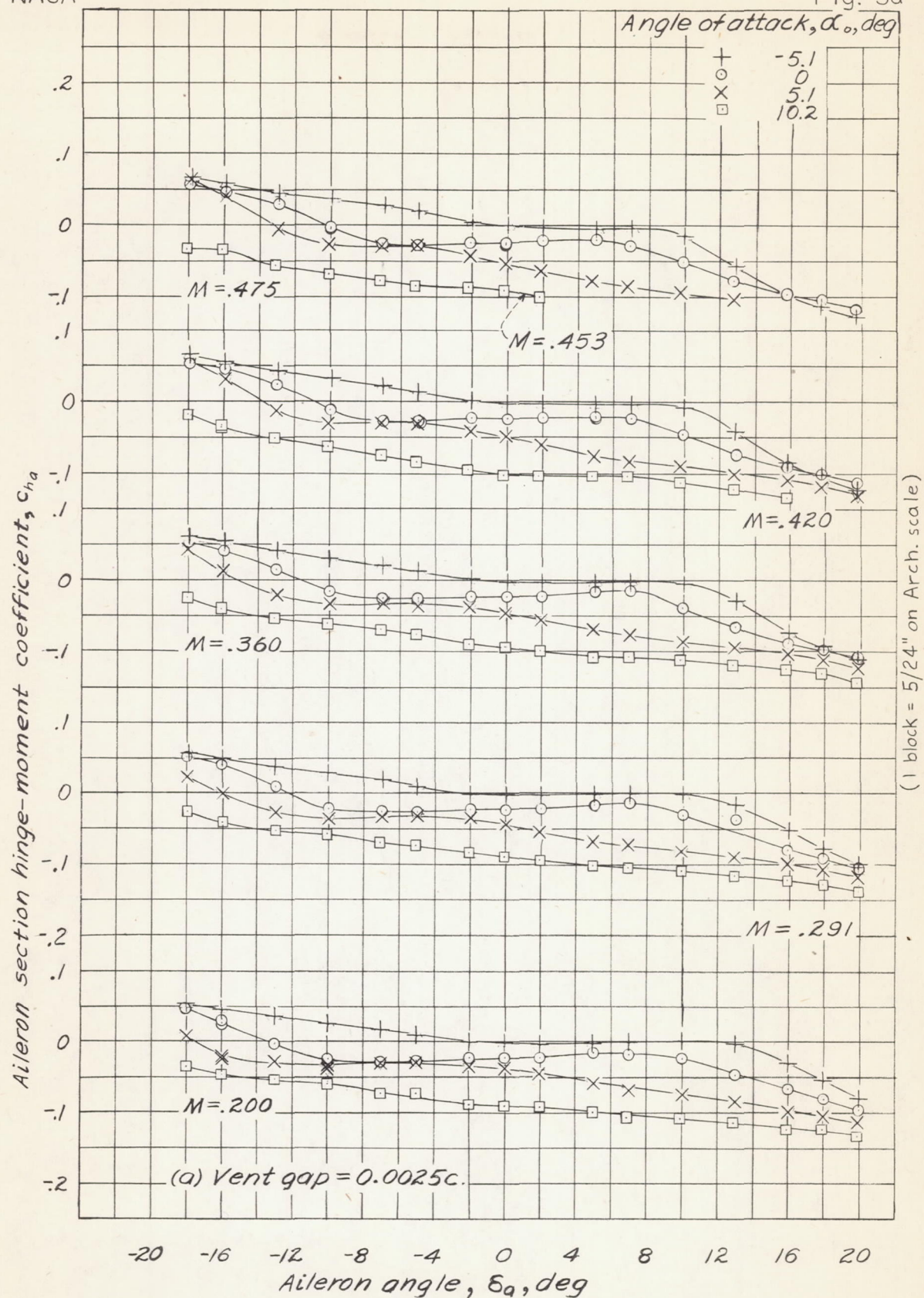


Figure 5. — Variation of aileron section hinge-moment coefficient with aileron angle.



NACA

Fig. 5b

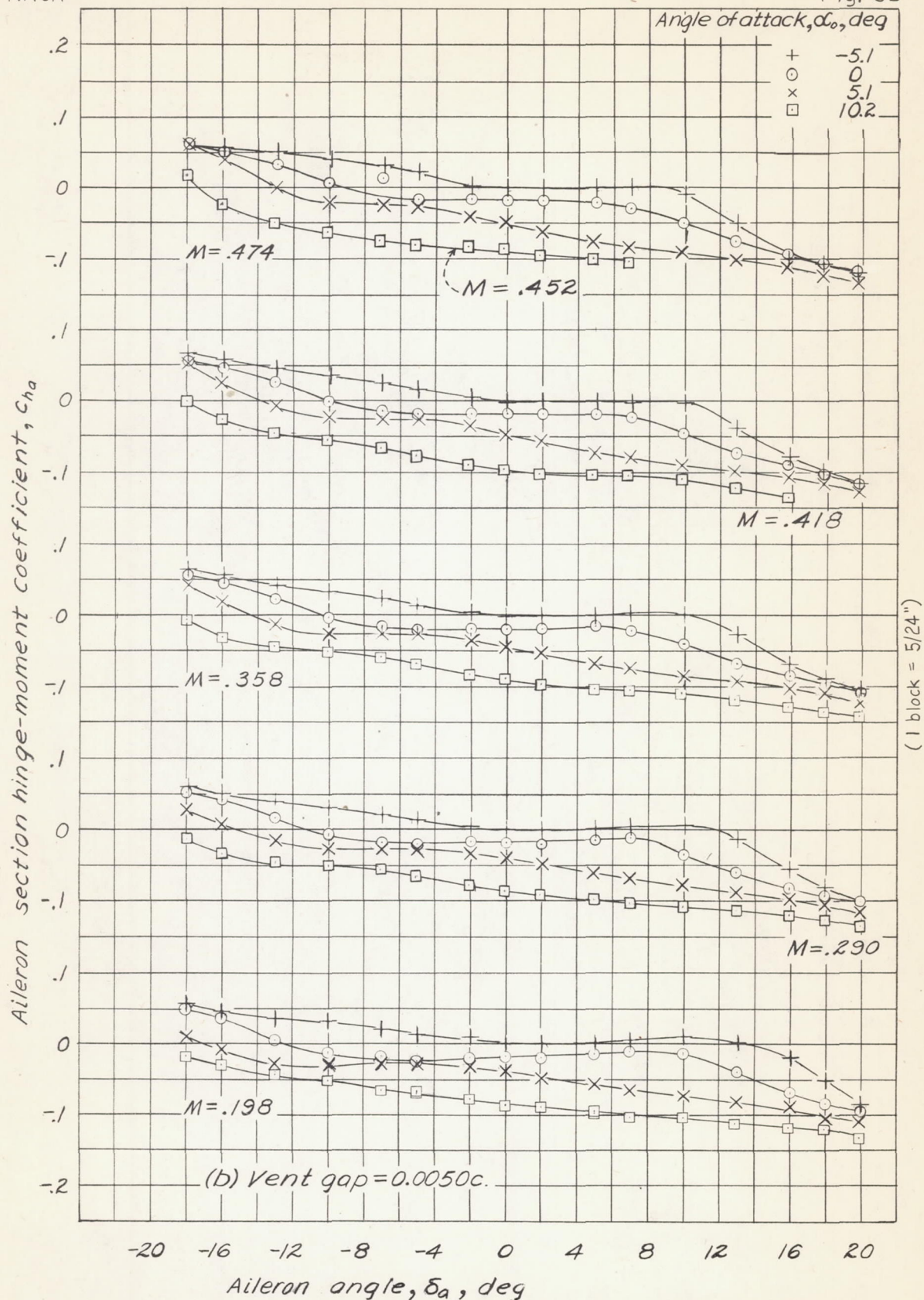
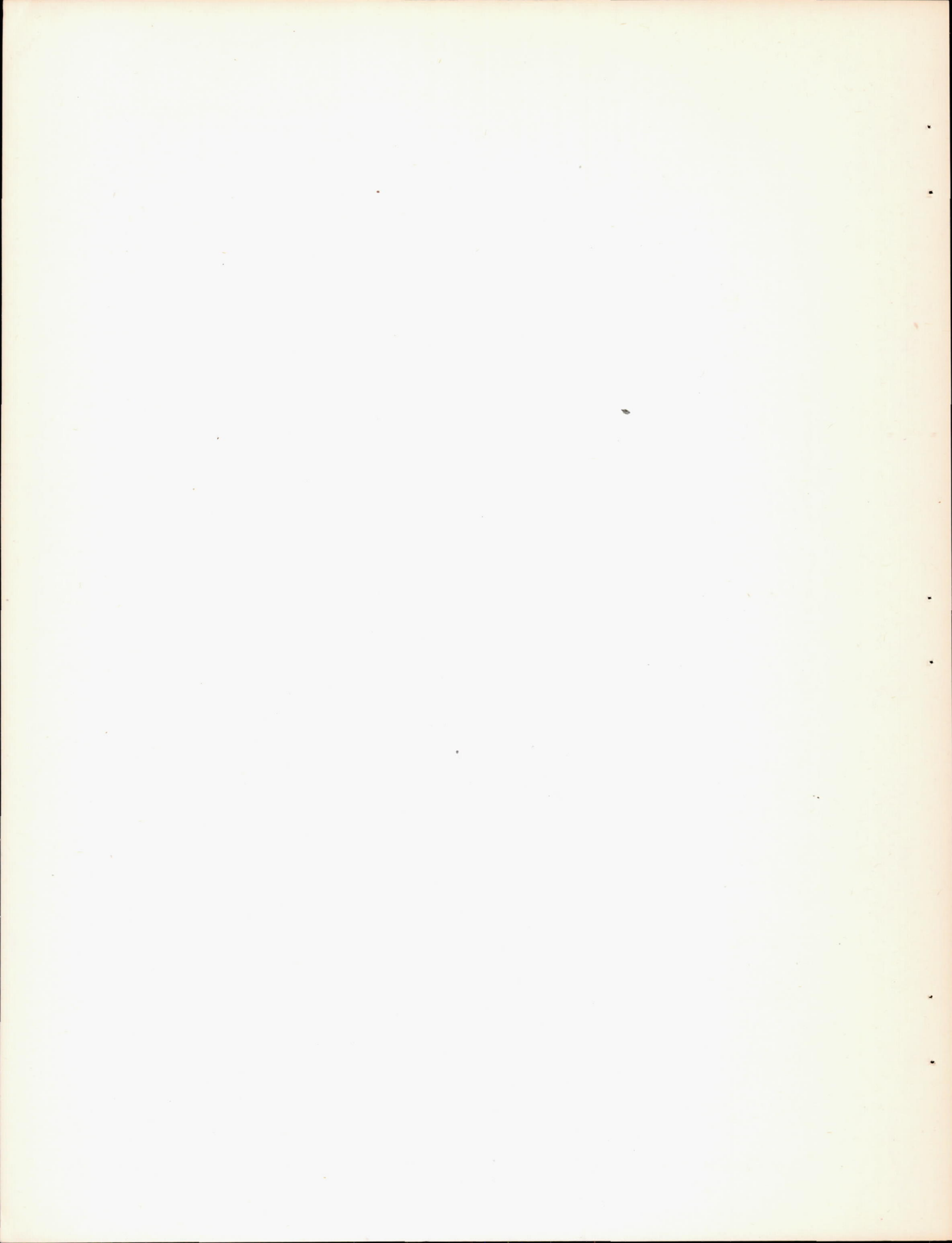


Figure 5. - Variation of aileron section hinge-moment coefficient with aileron angle. (Continued.)



NACA

Fig. 5c

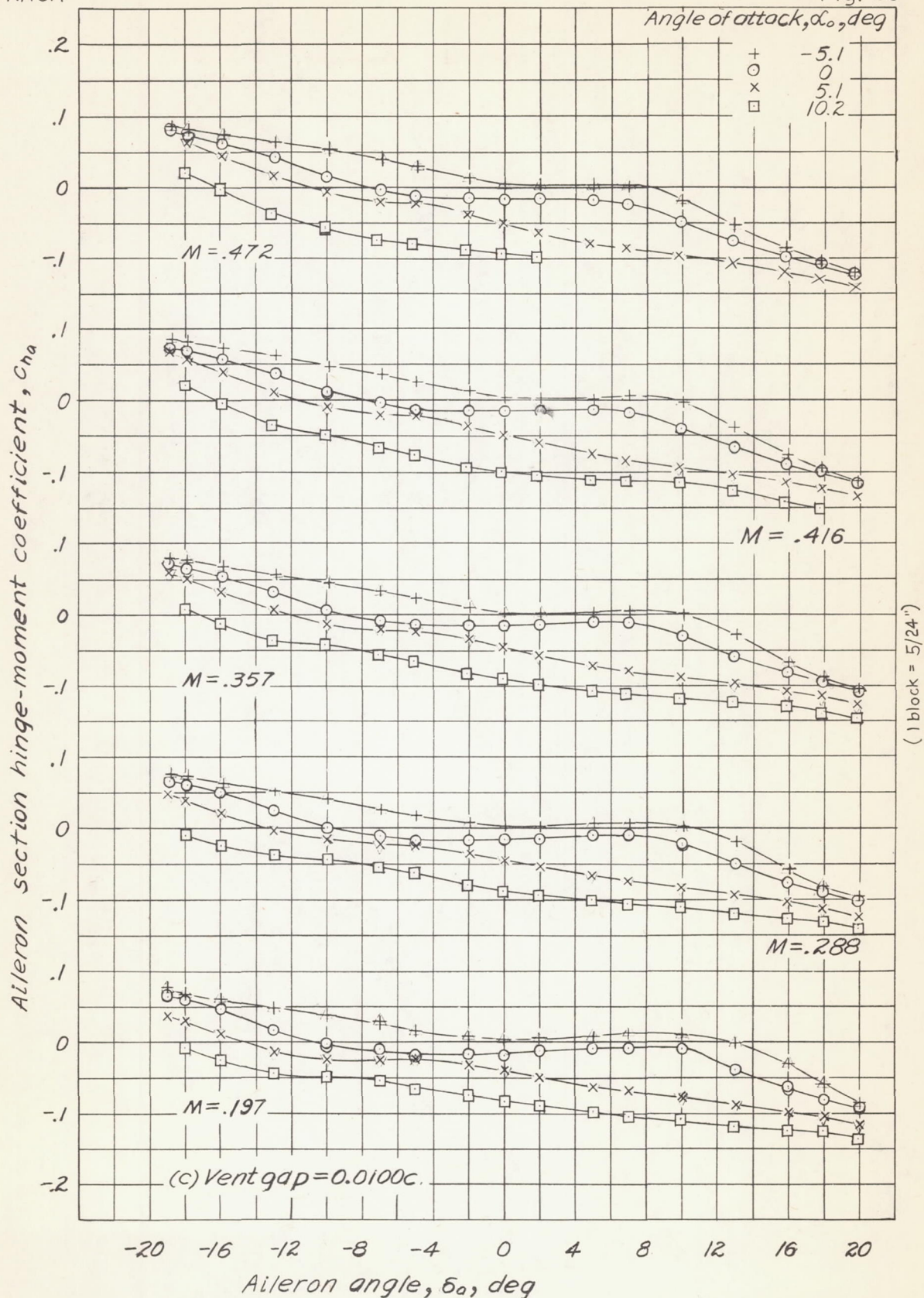


Figure 5. — Variation of aileron section hinge-moment coefficient with aileron angle. (Concluded.)



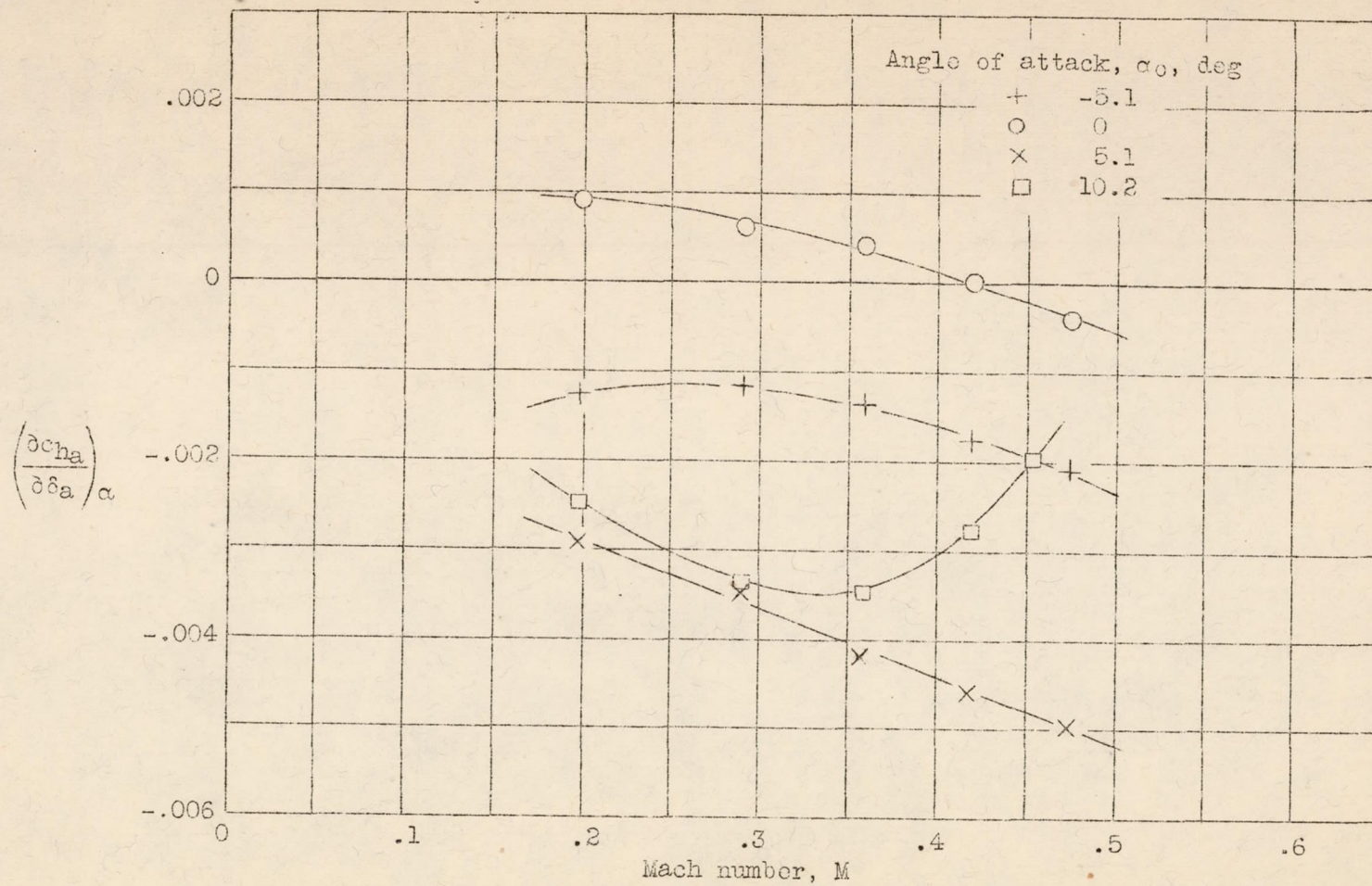


Figure 6.- Variation of the parameter  $(\partial ch_a / \partial \delta_a)\alpha$  with Mach number. Vent gap = 0.0055c.



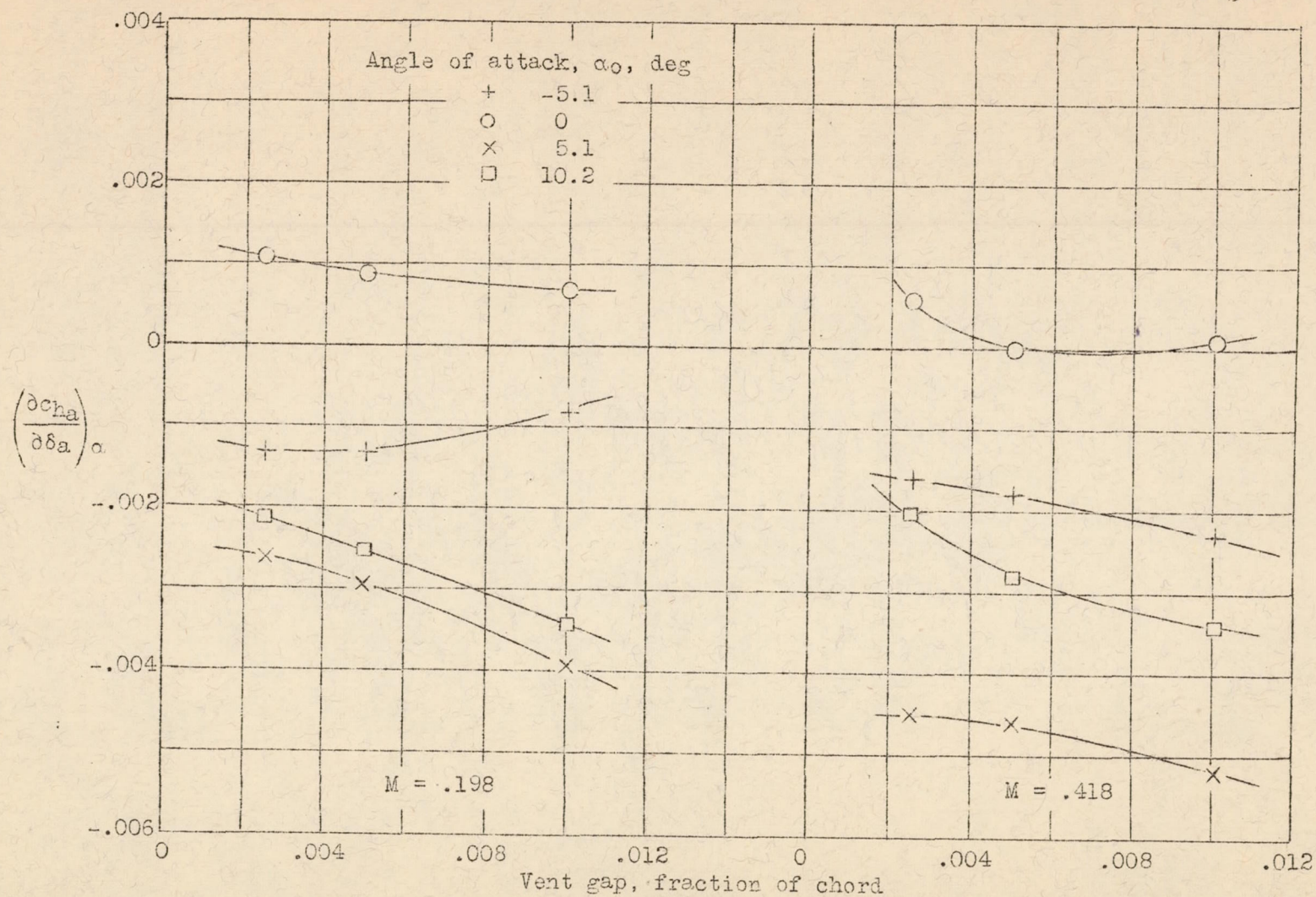


Figure 7.- Variation of the parameter  $(\partial c_{ha}/\partial \delta_a)\alpha$  with vent gap.



NACA

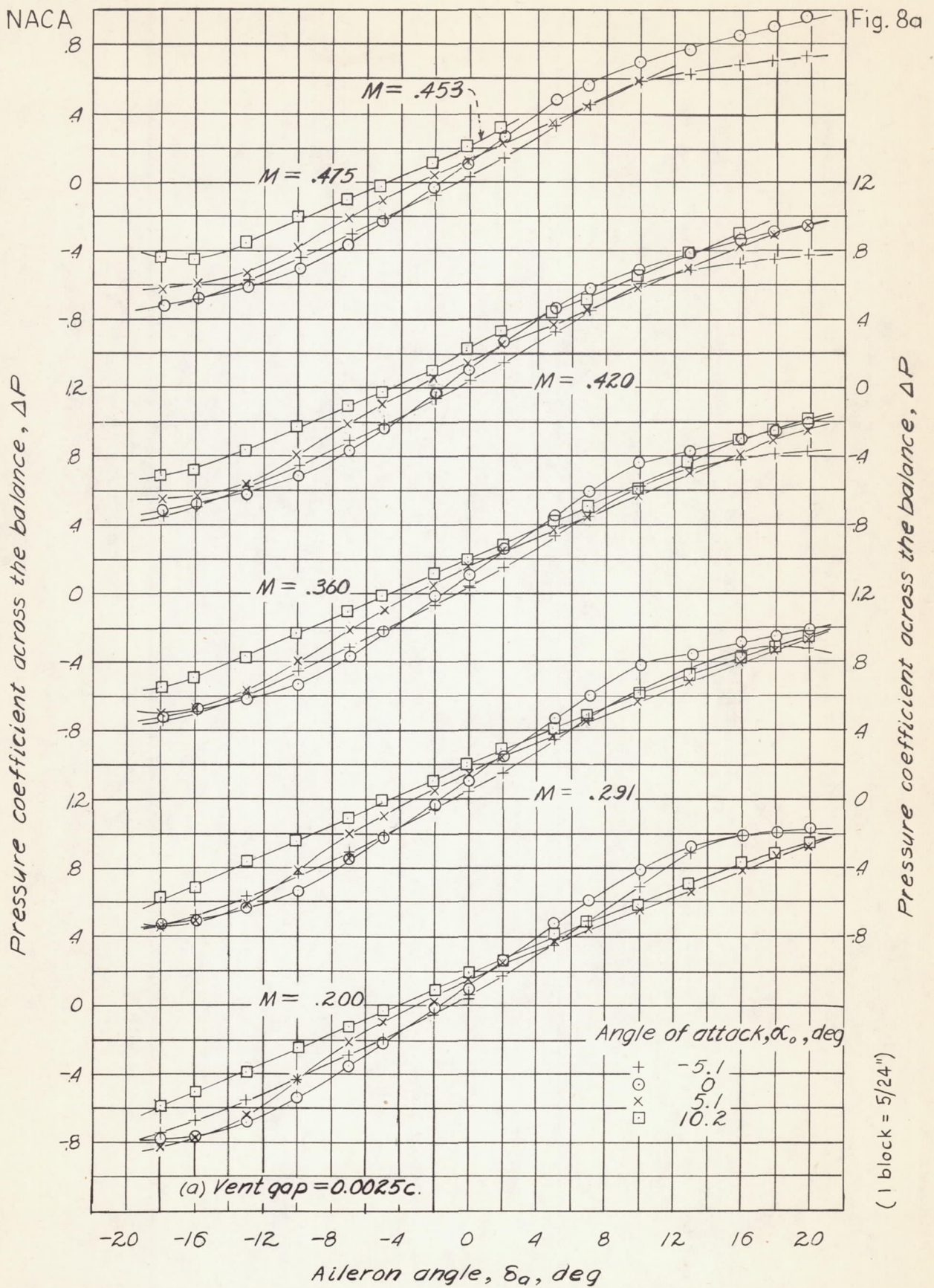


Figure 8. - Variation of pressure coefficient across the balance with aileron angle



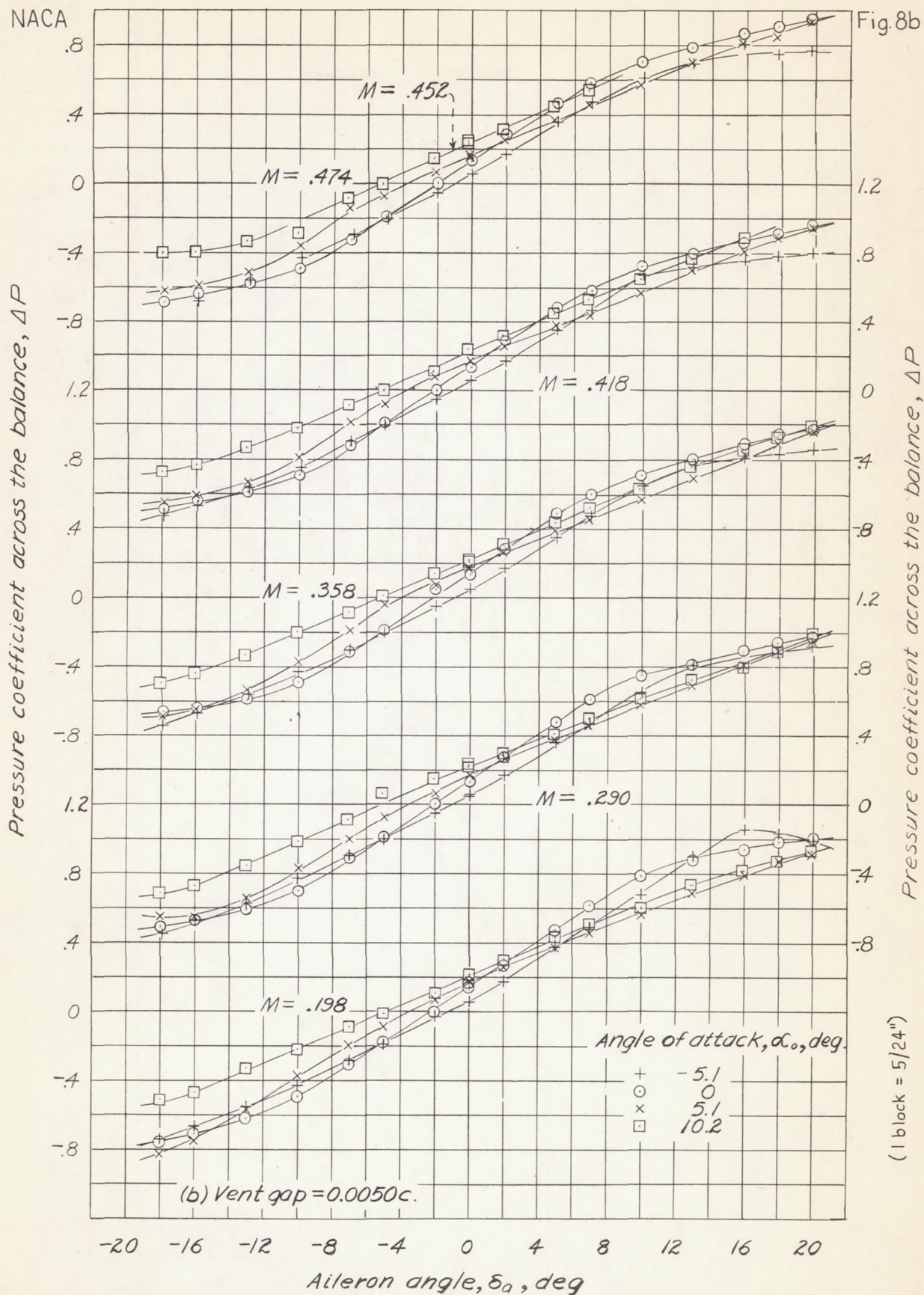


Figure 8. — Variation of pressure coefficient across the balance with aileron angle. (Continued.)



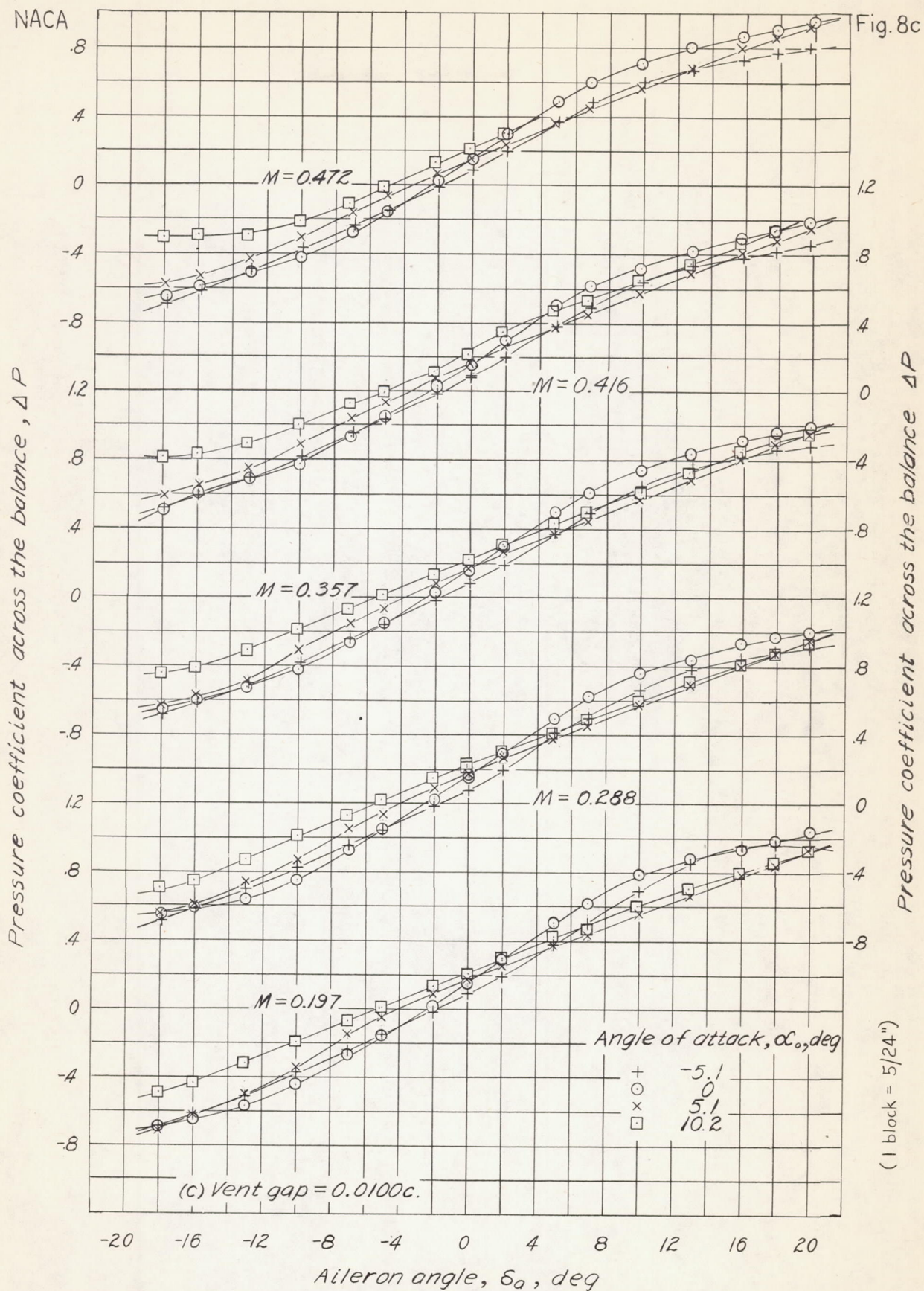
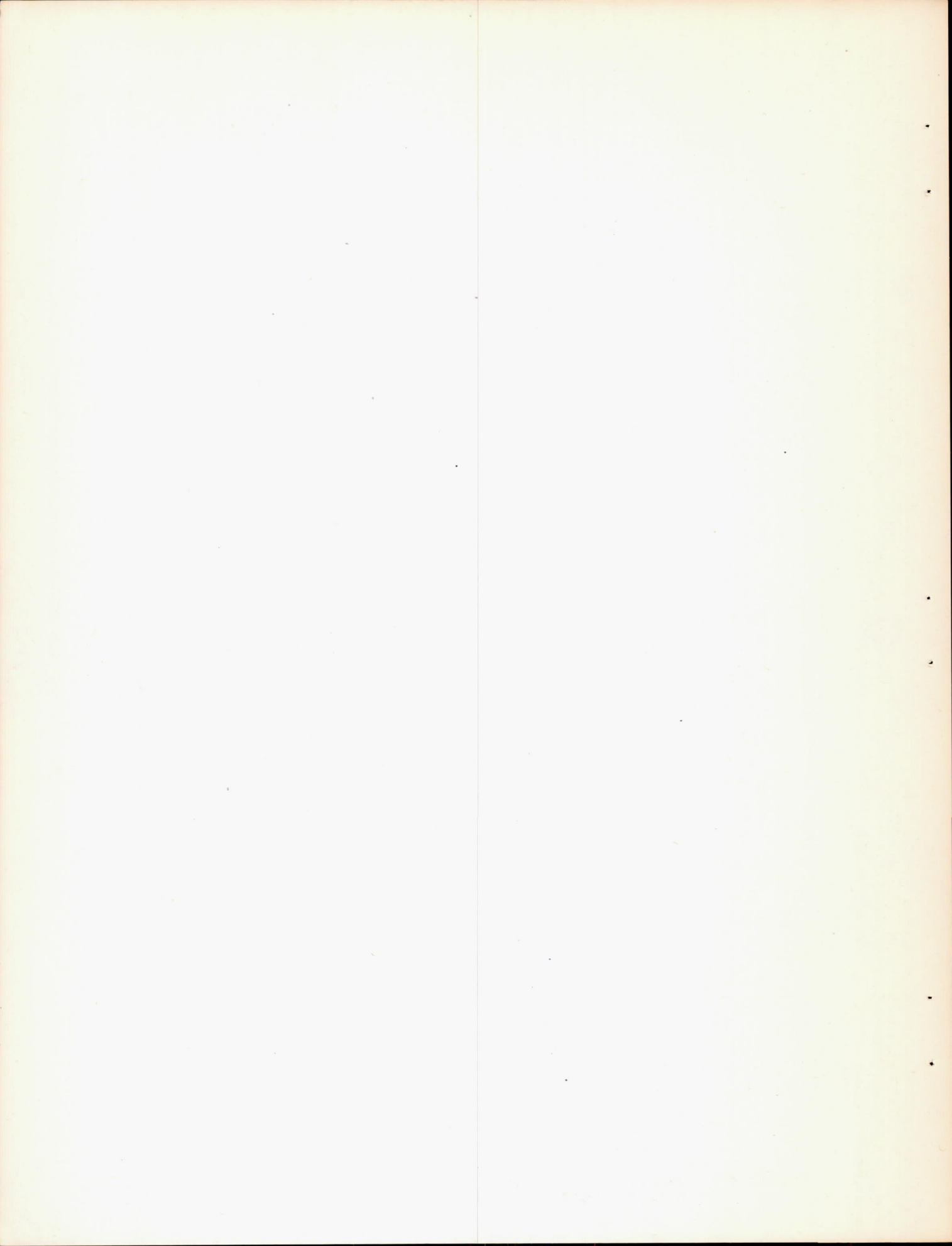


Figure 8. - Variation of pressure coefficient across the balance with aileron angle. (Concluded.)



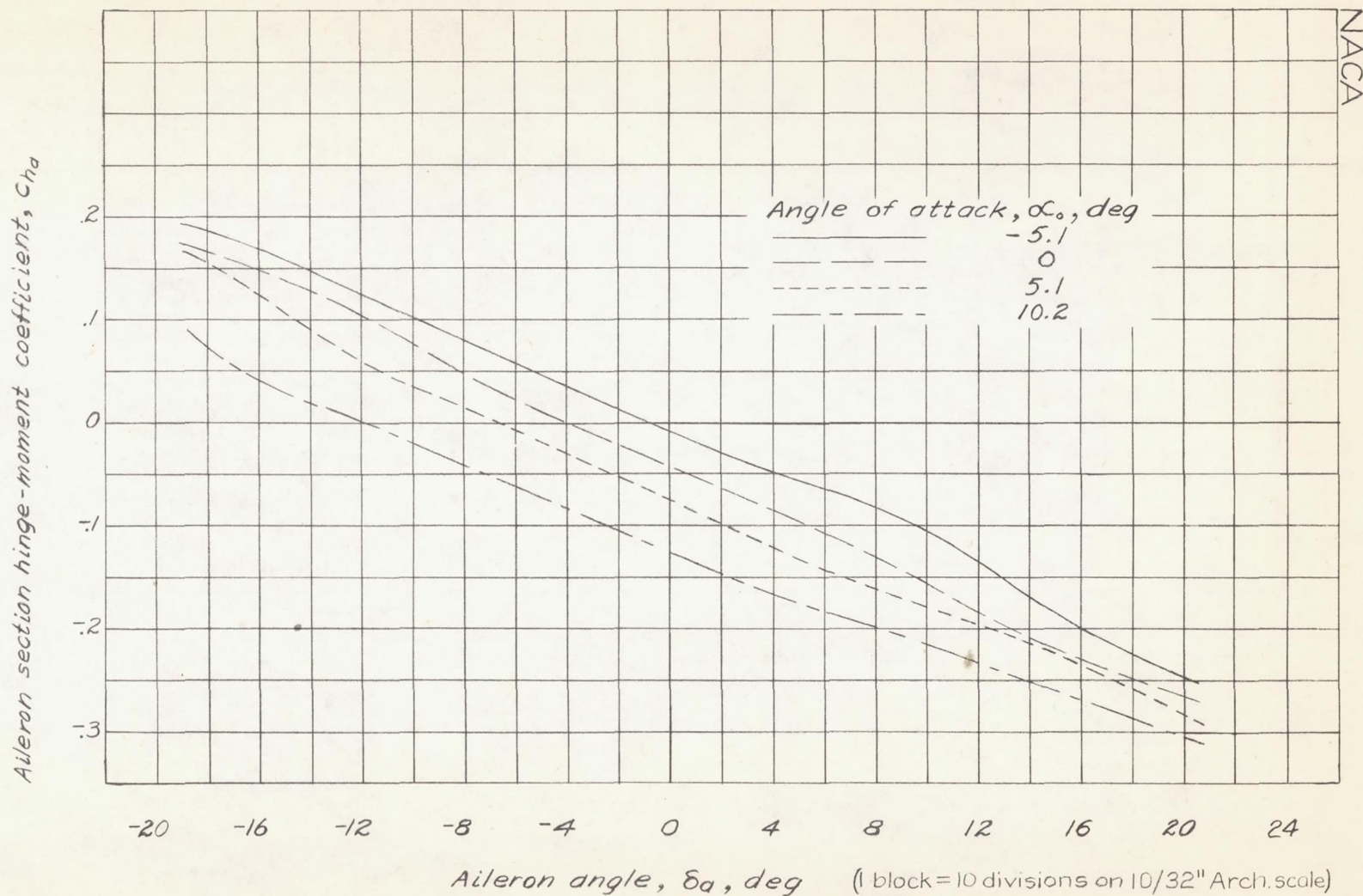


Figure 9. — Variation of  $C_{ha}$  with  $\delta_a$  for a 0.20c plain sealed aileron, computed from data on the 0.60c<sub>0</sub> internal balance aileron with vent gap = 0.005c.  $M=0.358$



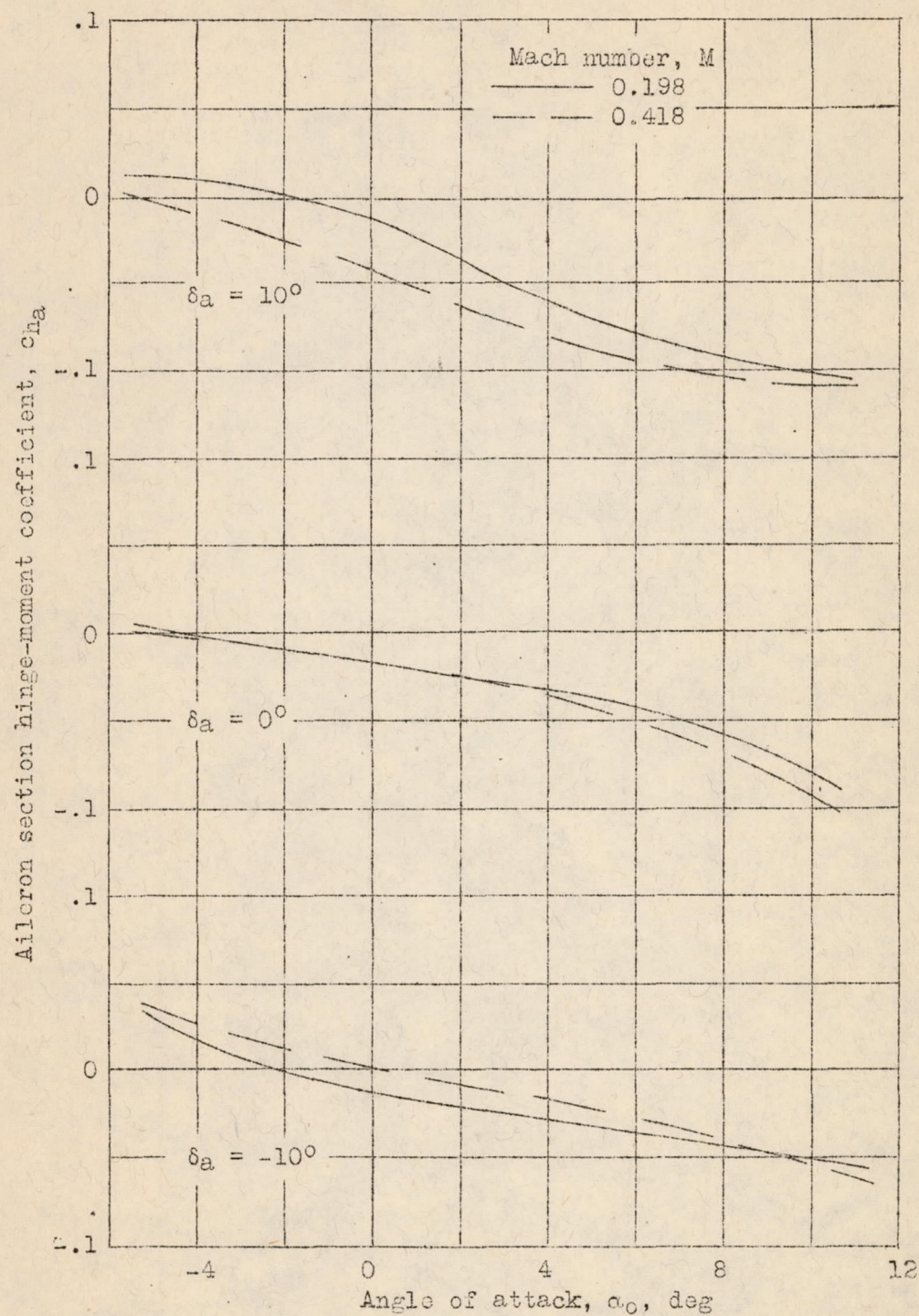


Figure 10.- Variation of  $c_{ha}$  with angle of attack. Vent gap = 0.0050c.

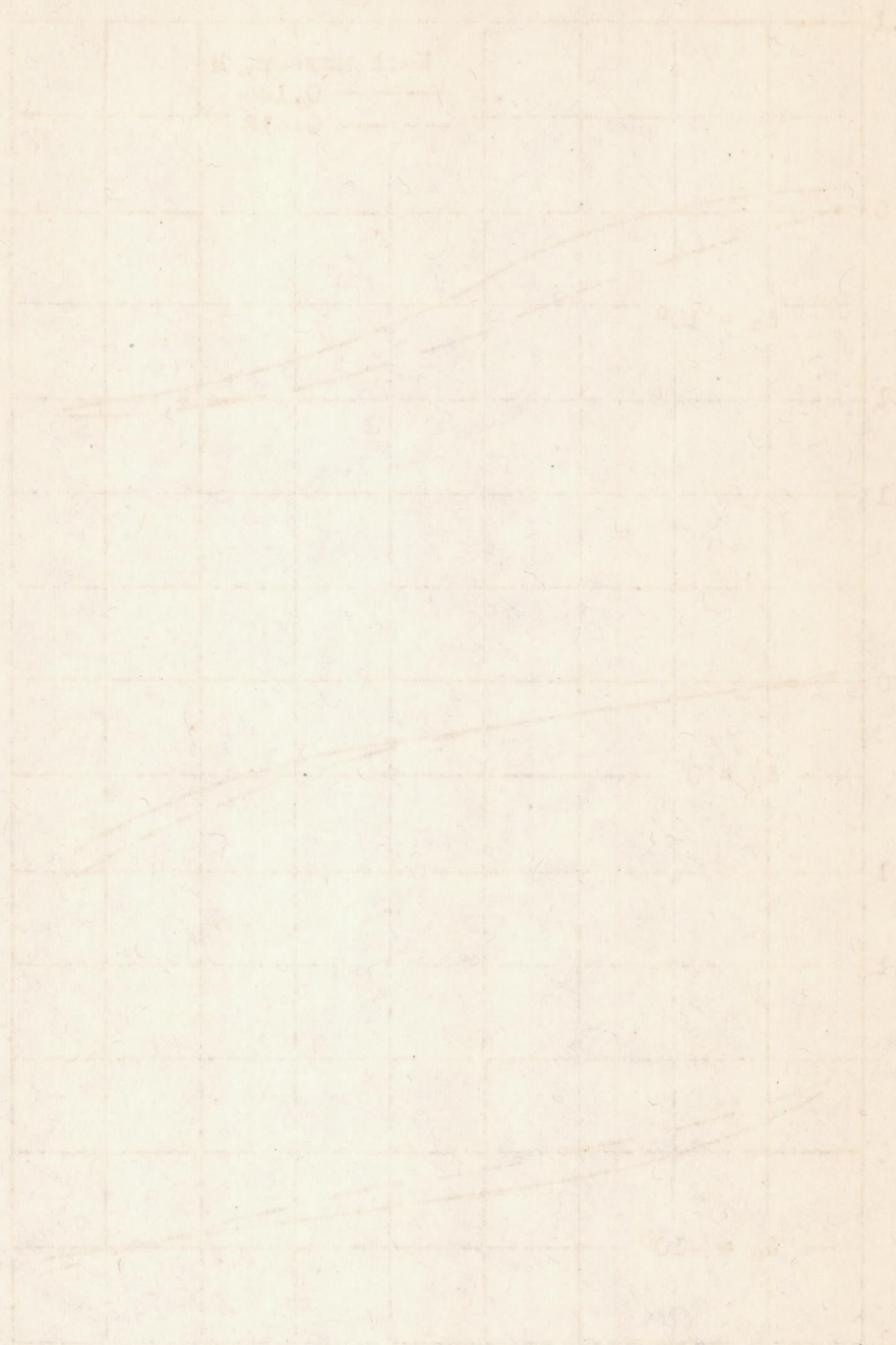


Fig. 10. - Graph of the function  $y = 100(1 - e^{-x})$  for  $x$  from 0 to 10. The curve is shown for  $y = 100(1 - e^{-x})$  and  $y = 50(1 - e^{-x})$  and  $y = 25(1 - e^{-x})$ .

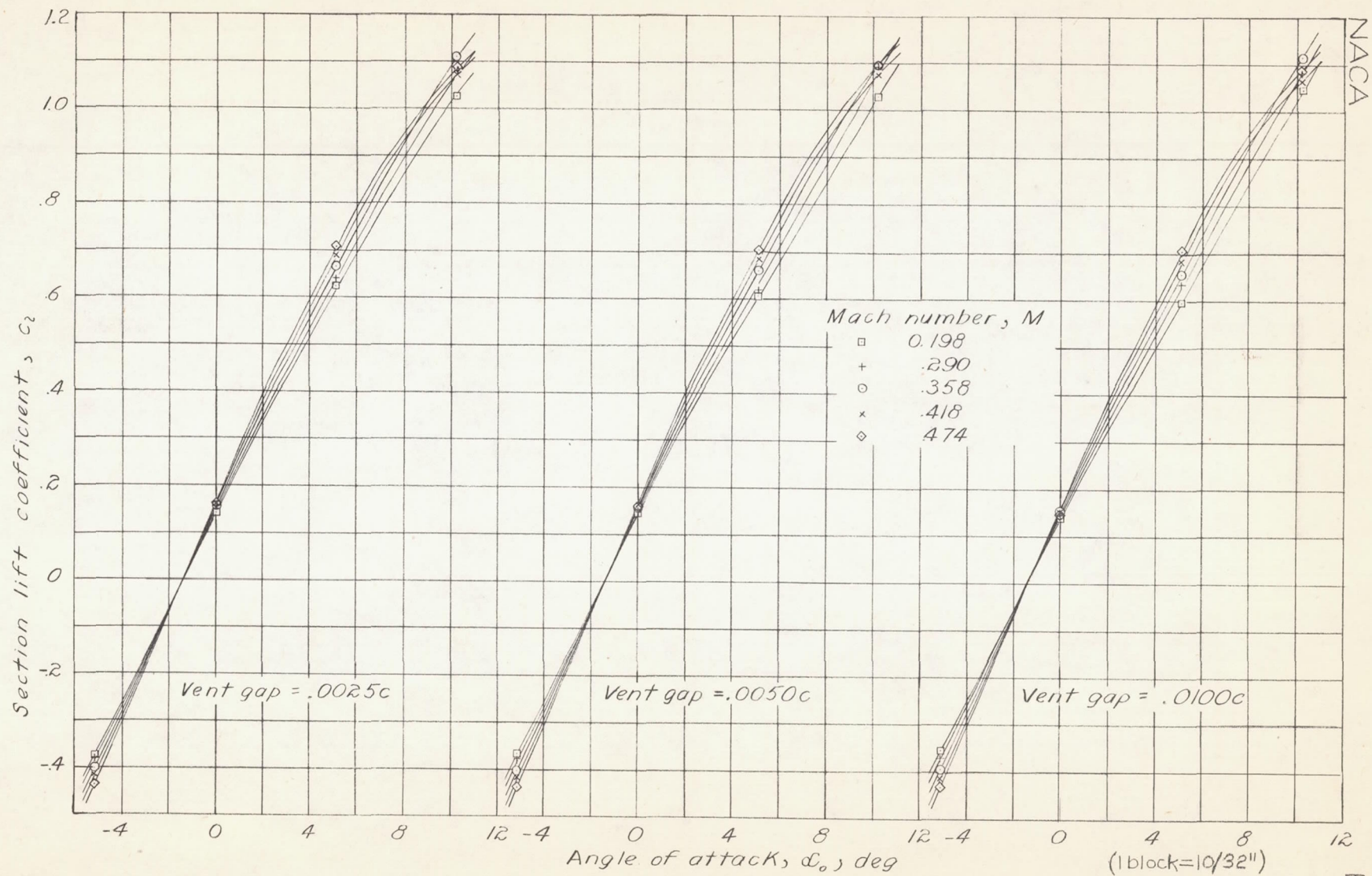


Figure 11. — Variation of section lift coefficient with angle of attack,  $\delta_a = 0^\circ$ .



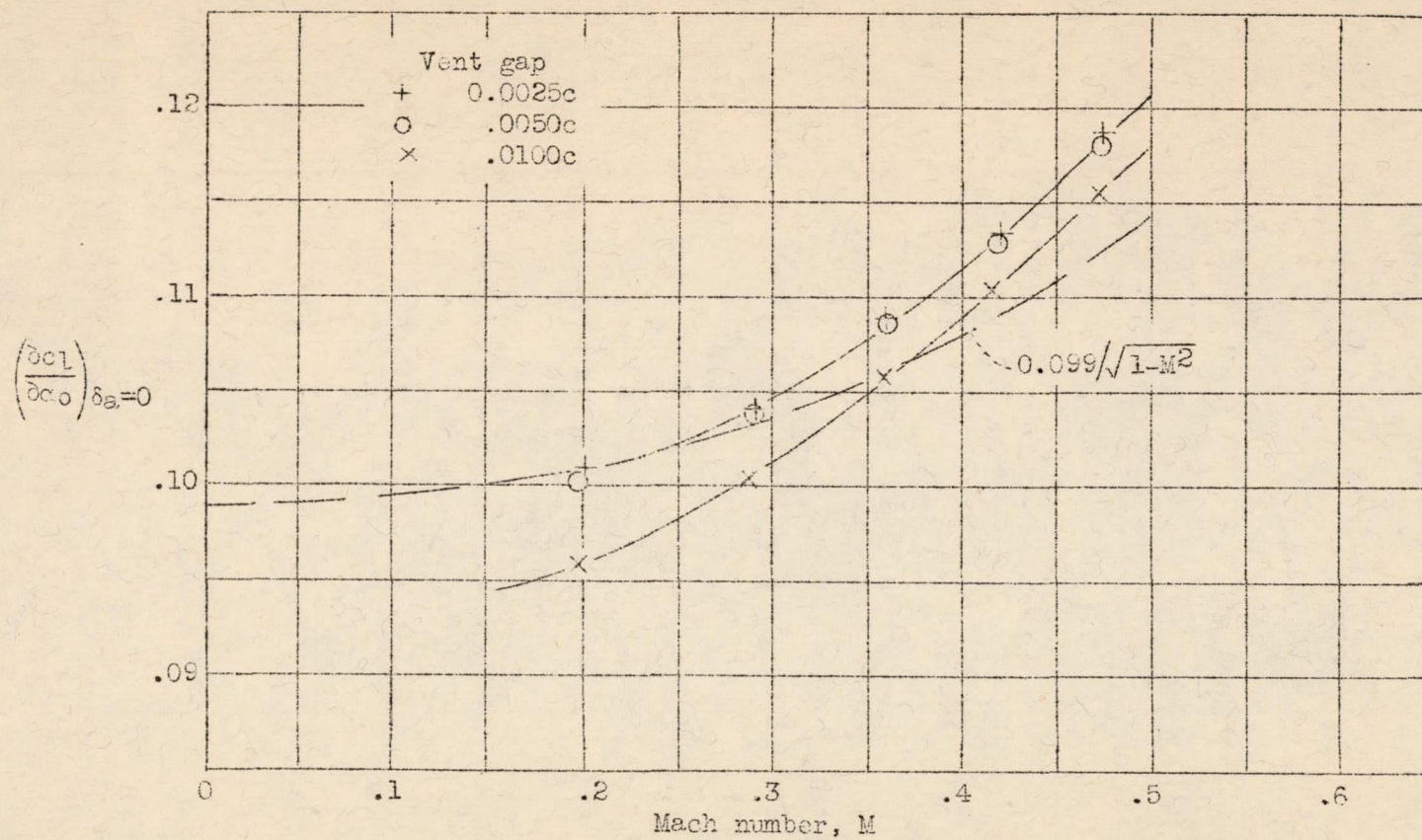
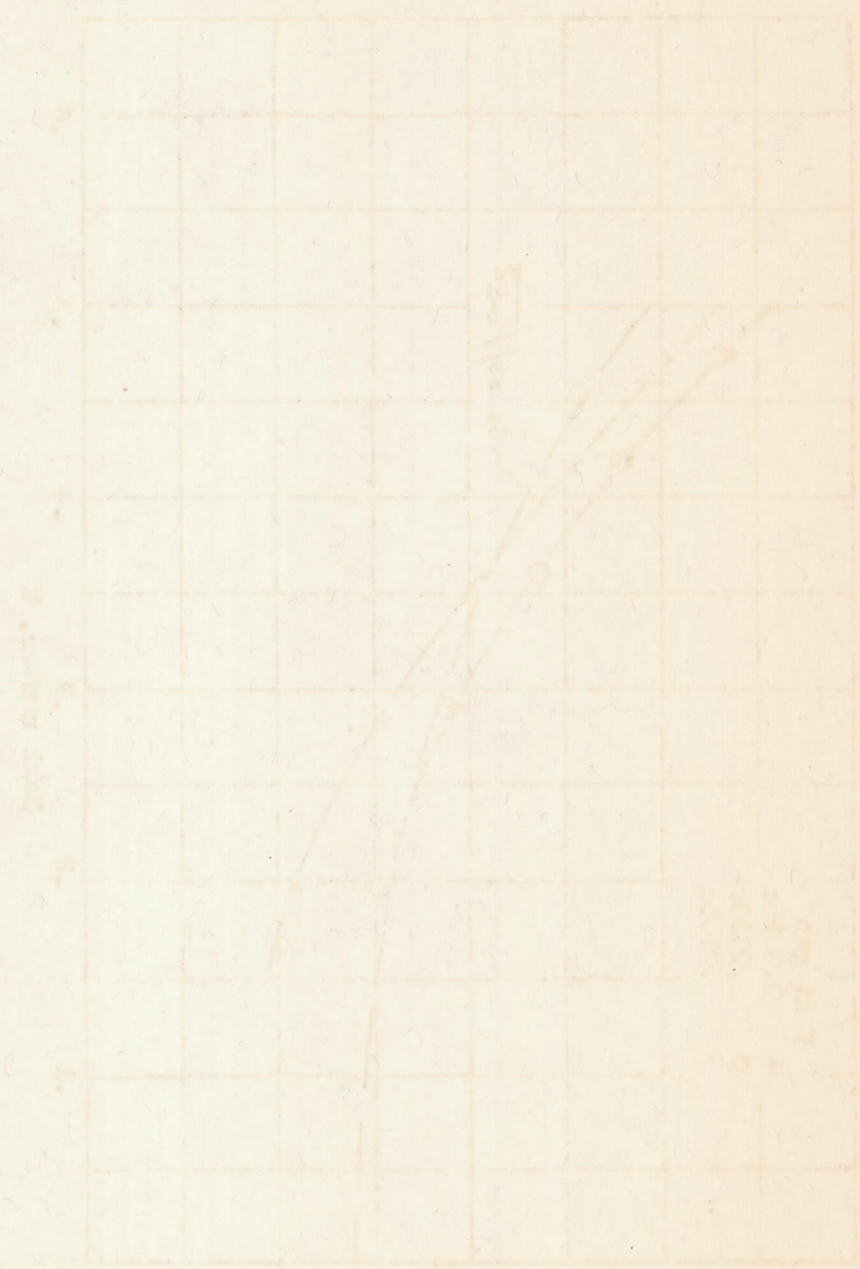


Figure 12.- Variation of the parameter  $(\partial c_l/\partial \alpha_0)_{\delta=0}$  with Mach number.

SE 45

ADAM

1. The first of the three lines is a straight line passing through the origin and the point (10, 10).



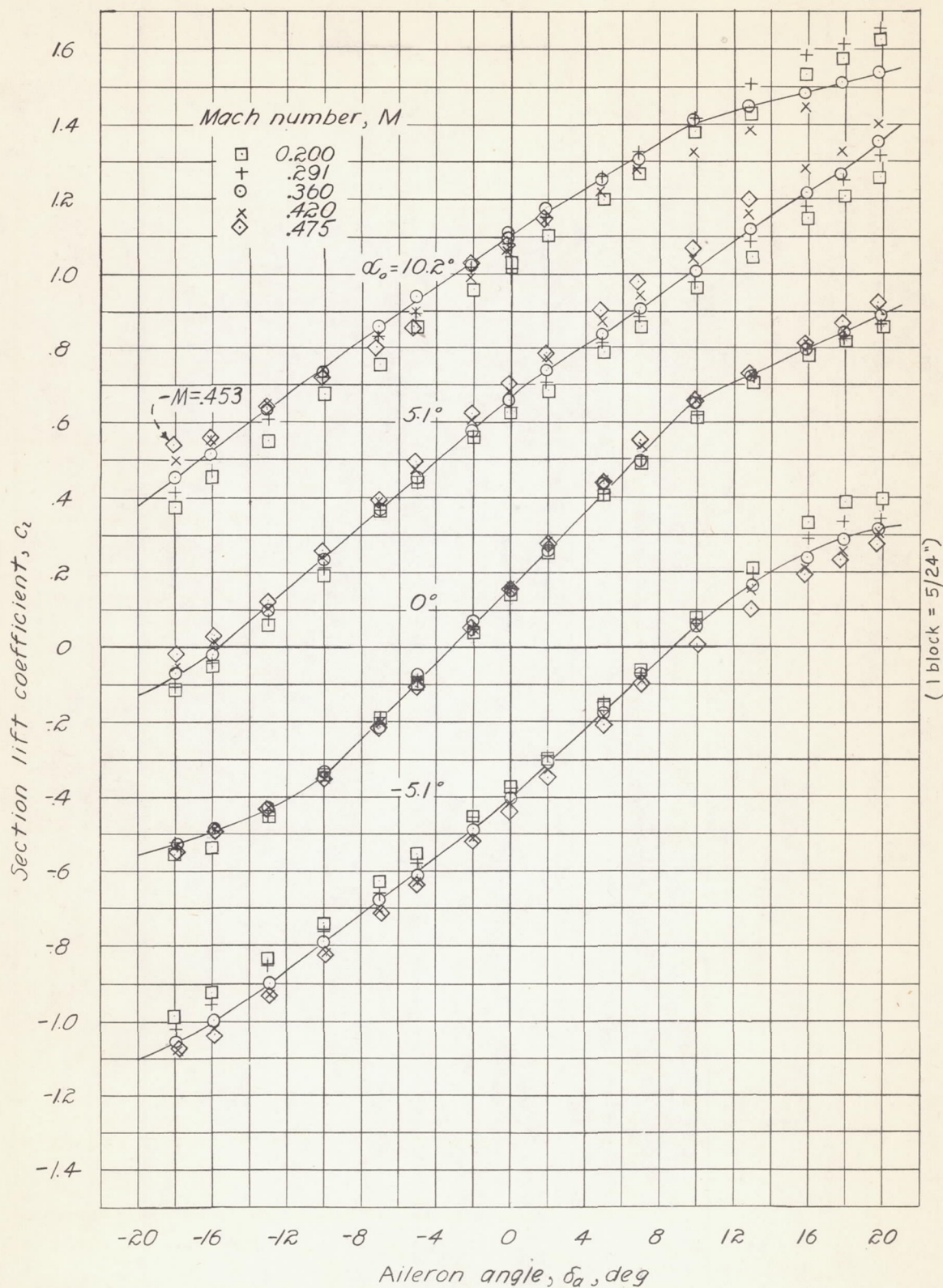
10

10

10

10

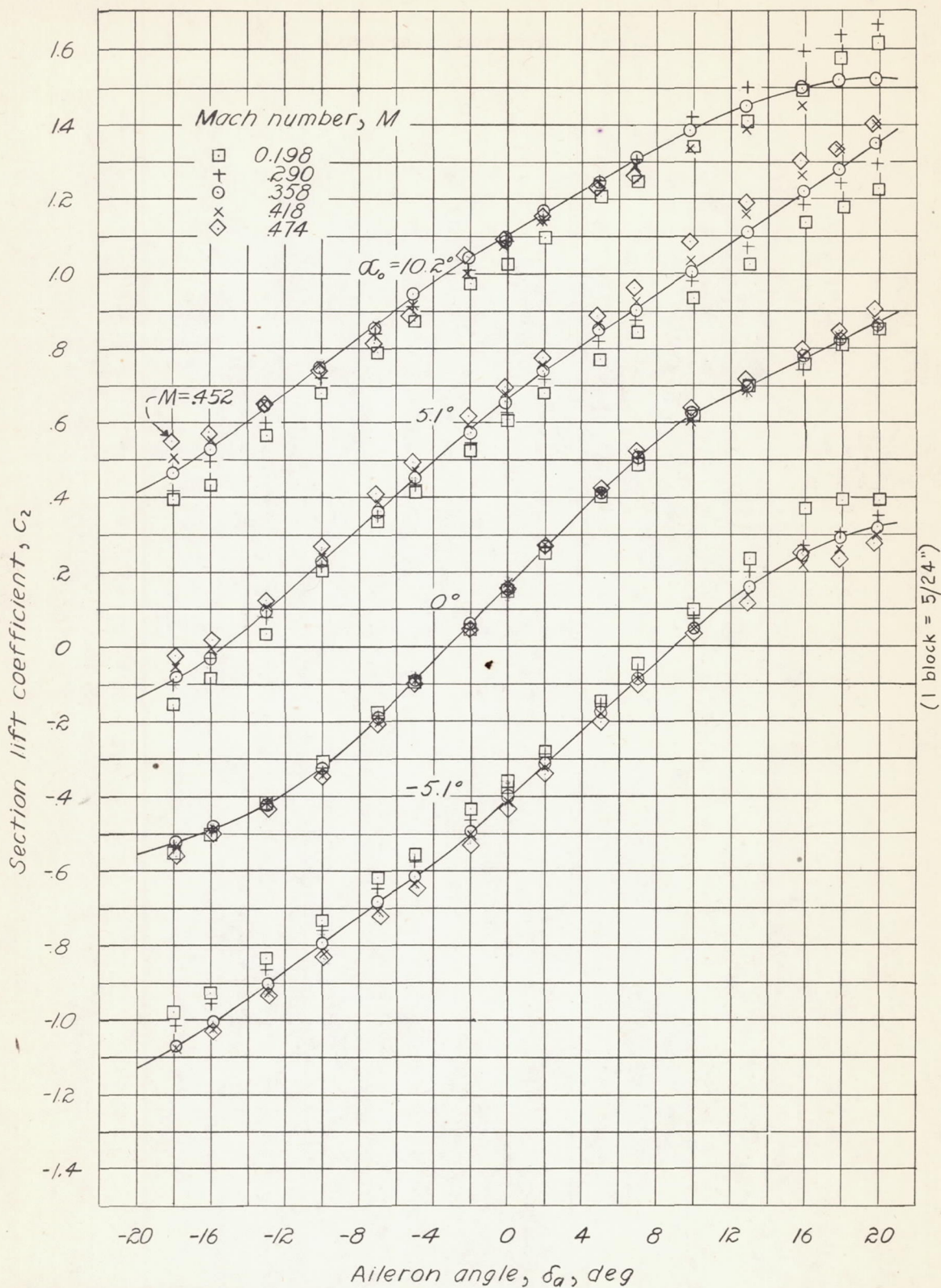
10



(a) Vent Gap = 0.0025c.

Figure 13. - Variation of section lift coefficient with aileron angle.

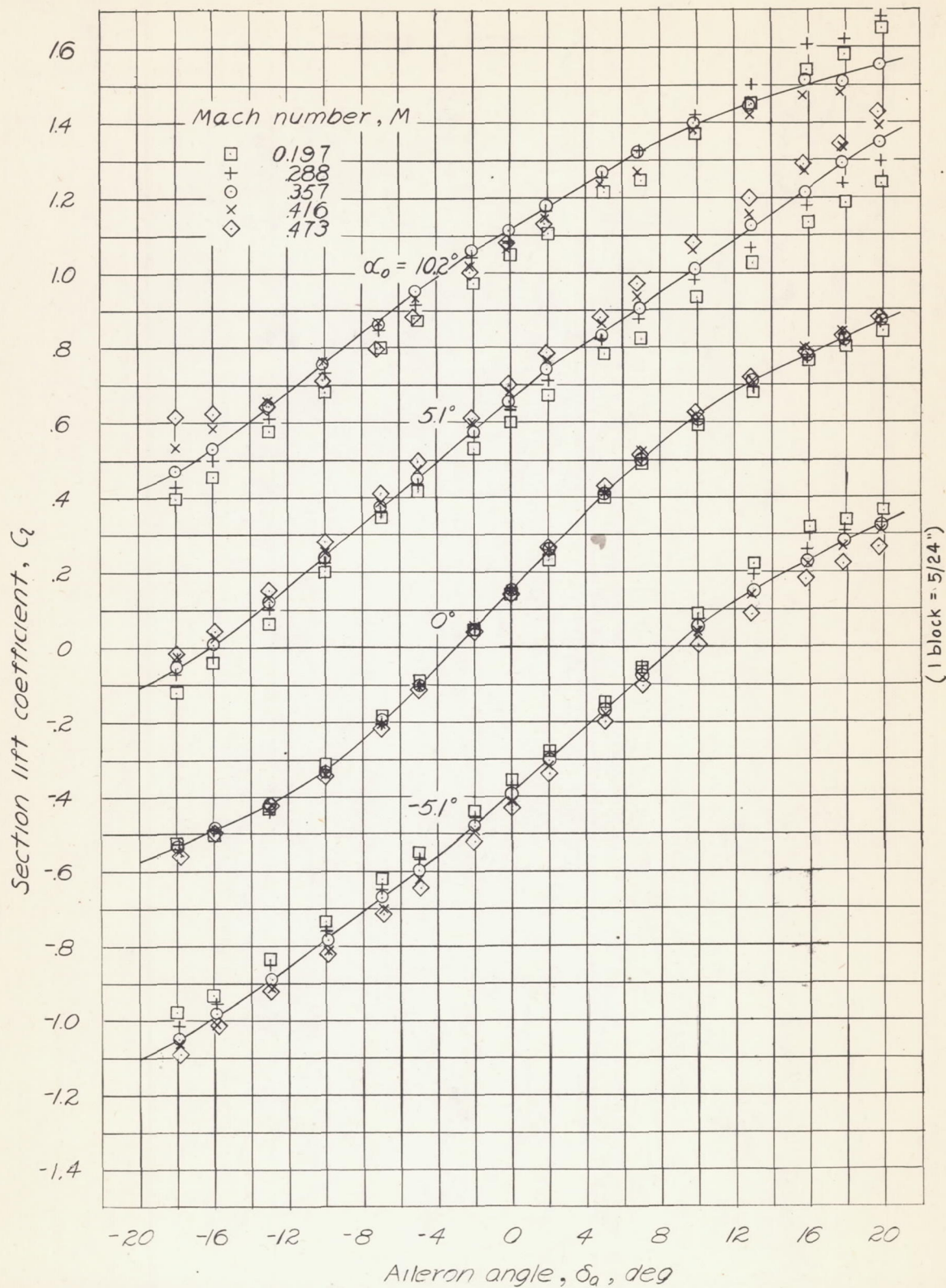




(b) Vent Gap = 0.0050c.

Figure 13. - Variation of section lift coefficient with aileron angle.  
(Continued.)





(a) Vent Gap = 0.0100c.

Figure 13. - Variation of section lift coefficient with aileron angle.  
(Cont'd. 1.)



L-432

NACA

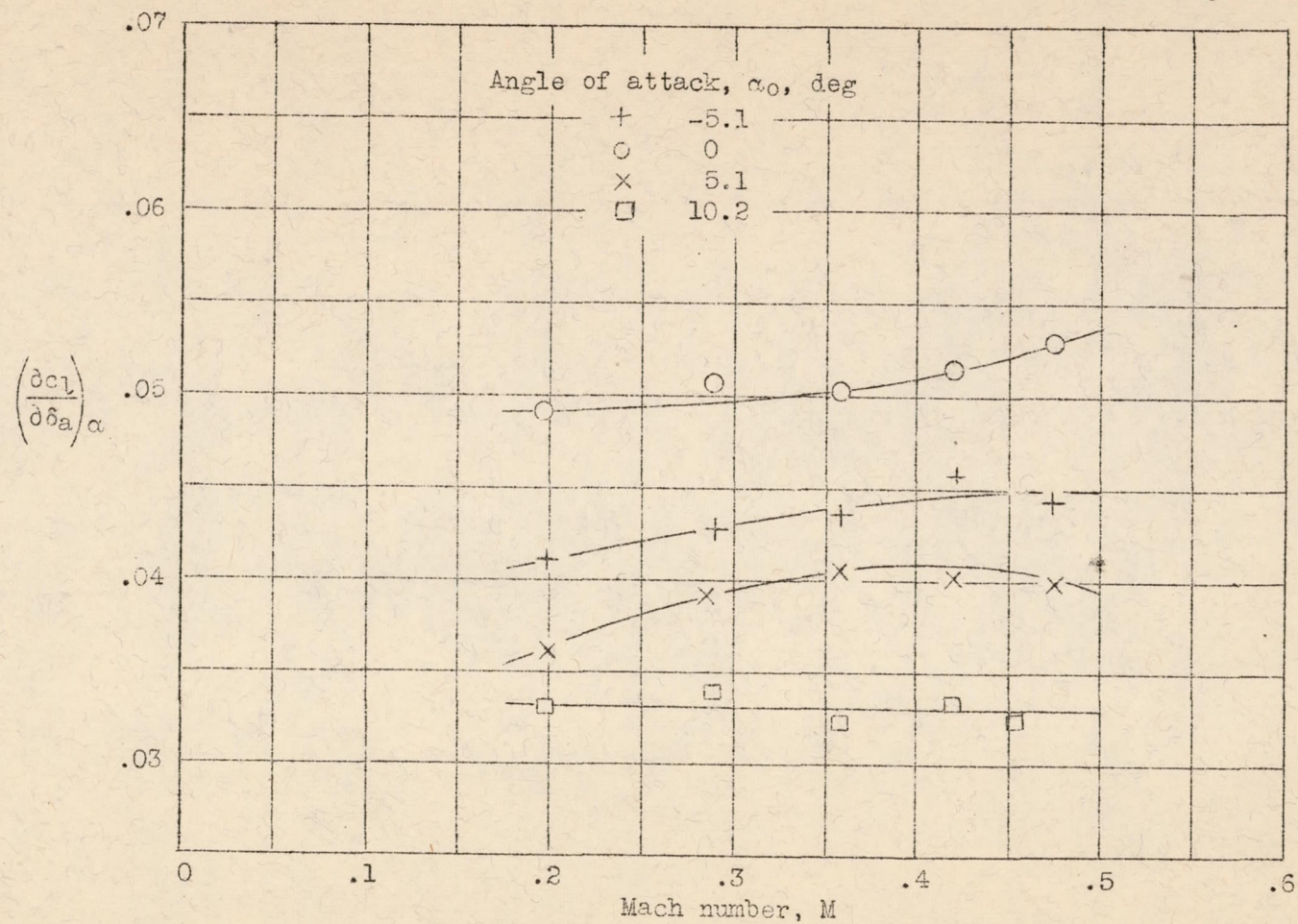


Figure 14.- Variation of the parameter  $(\partial c_l / \partial \delta_a)\alpha$  with Mach number. Vent gap = 0.0050c.

Fig. 14



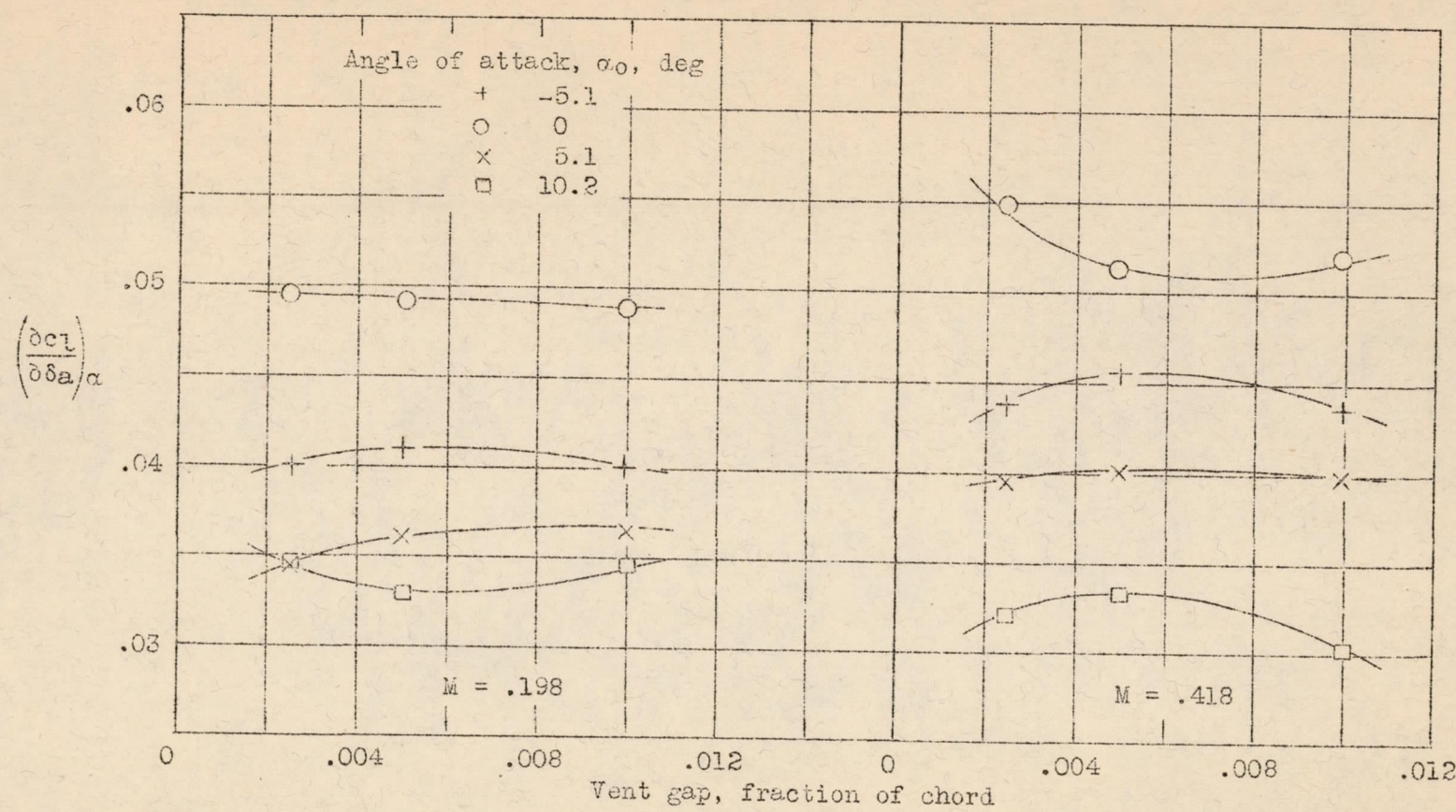
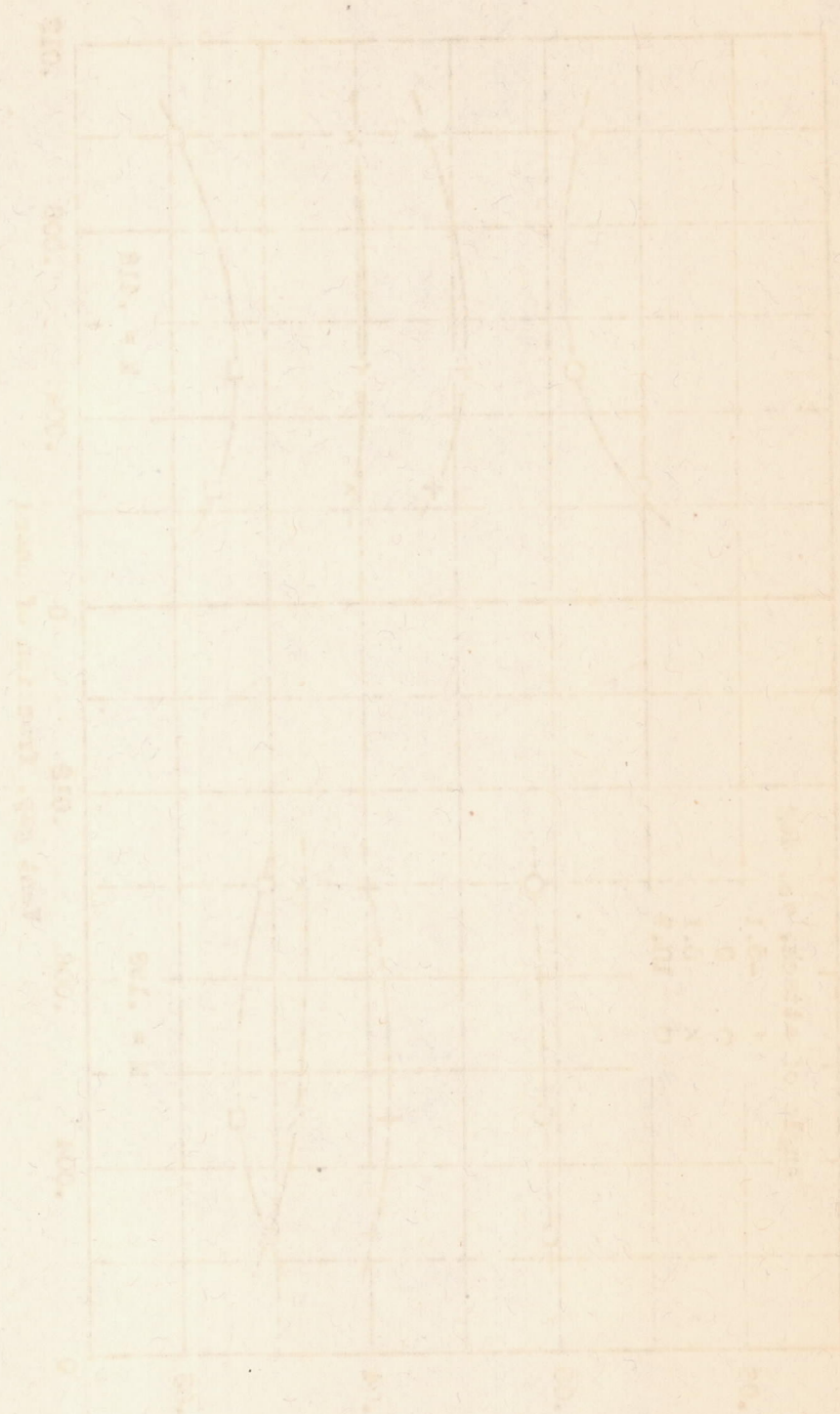


Figure 15.- Variation of the parameter  $(\partial c_l / \partial \delta_a) \alpha$  with vent gap.

Fig. 1. The dependence of the critical current density  $J_{c0}$  on the magnetic field  $H$  for different values of the parameter  $\alpha$ .



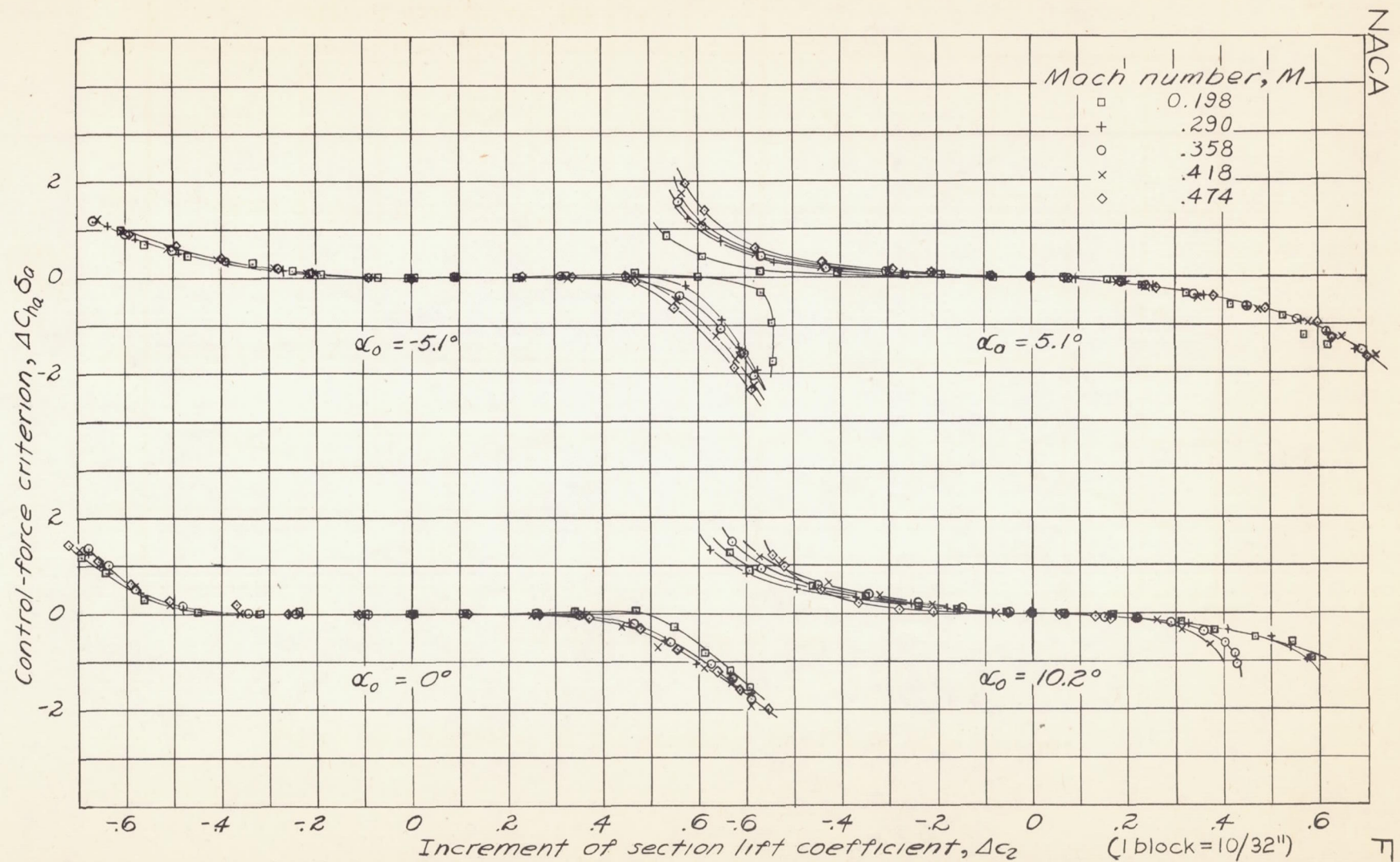


Figure 16. — Variation of control-force criterion with increment of section lift coefficient,  $\Delta c_2$  showing effect of Mach number. Vent gap = 0.0050c.



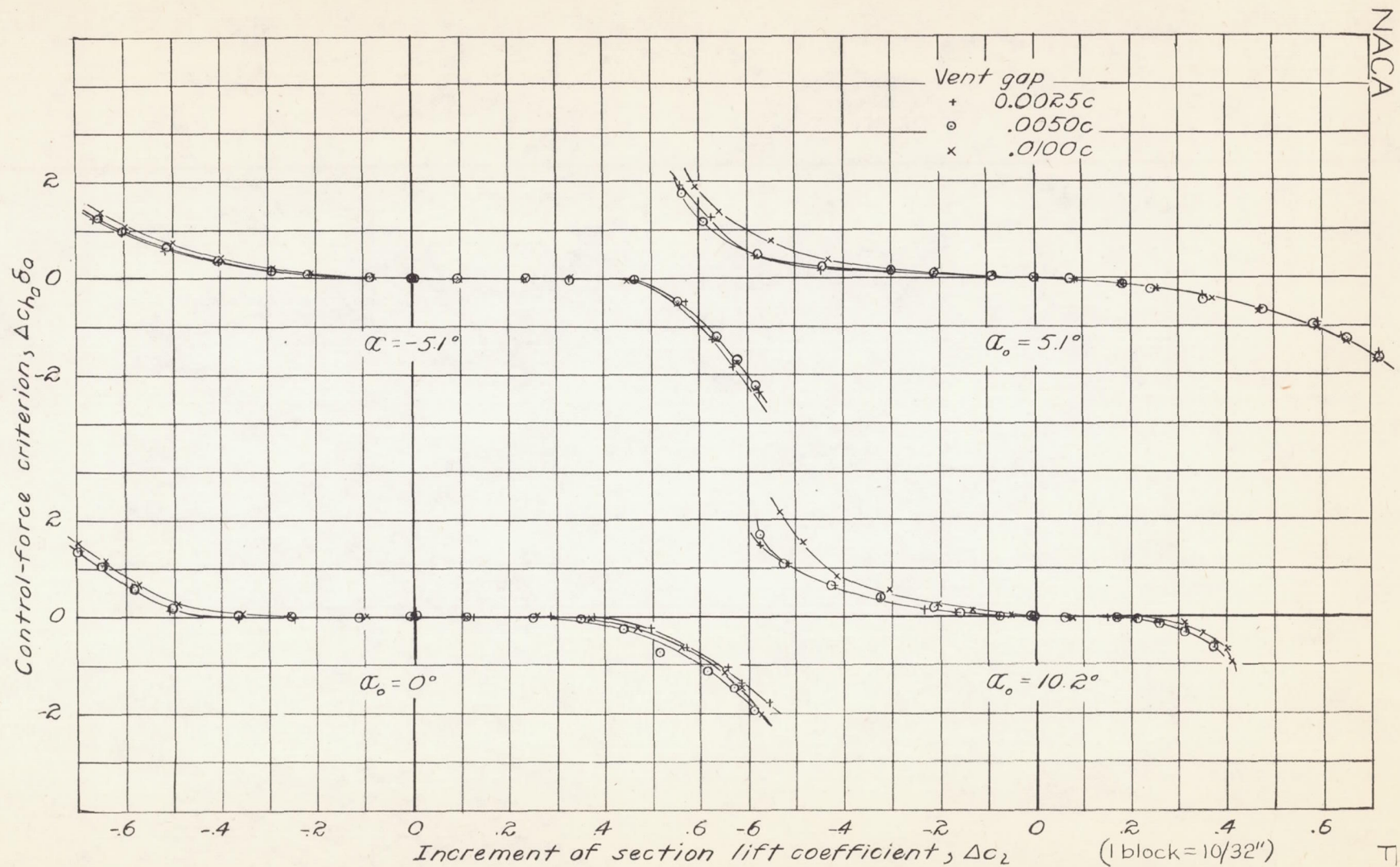


Figure 17. — Variation of control-force criterion with increment of section lift coefficient, showing effect of vent gap.  $M = 0.418$ .



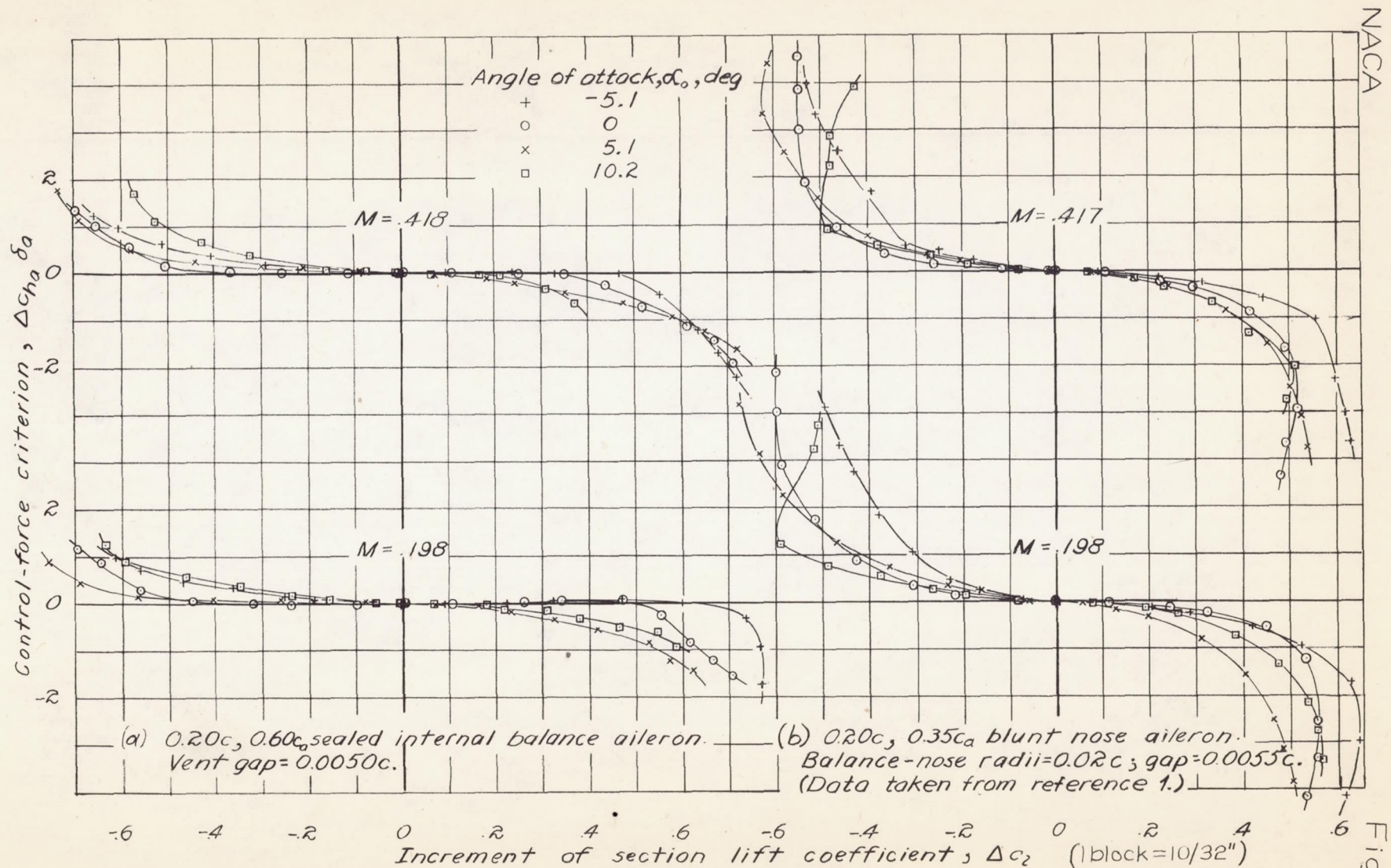


Figure 18.— Variation of  $\Delta c_h \delta_a$  with  $\Delta c_2$ , showing a comparison of sealed internal balance aileron tested and a blunt nose aileron, reported in reference 1, on the same airfoil.